New yrast and non-yrast states in ^{136}I and medium-spin structure of ^{136}I and ^{136}Xe: Roles of the proton $d_{5/2}$ and the neutron $h_{9/2}$ orbitals beyond ^{132}Sn

R. Lozeva,[1,2,3,*] E. A. Stefanova,[4] H. Naïdja,[2,3,5] F. Nowacki,[2,3] T. Rząca-Urban,[6] J. Wisniewski,[6] W. Urban,[6] I. Ahmad,[7] A. Blanc,[8] G. De France,[9] F. Didierjean,[2,3] G. Duchêne,[2,3] H. Faust,[8] J. P. Greene,[7] U. Köster,[8] P. Mutti,[8] G. Simpson,[10] A. G. Smith,[11] T. Soldner,[8] and C. A. Ur[12]

[1]*CSNSM, CNRS/IN2P3, Université Paris-Sud, F-91405 Orsay Campus, France*
[2]*Université de Strasbourg, IPHC, 23 rue du Loess, F-67037 Strasbourg, France*
[3]*CNRS, UMR 7178, F-67037 Strasbourg, France*
[4]*INRNE, BAS, BG-1784 Sofia, Bulgaria*
[5]*University of Constantine, 25000 Constantine, Algeria*
[6]*Faculty of Physics, University of Warsaw, PL-02093 Warsaw, Poland*
[7]*Argonne National Laboratory, Argonne, Illinois 60439, USA*
[8]*ILL, F-38000 Grenoble Cedex 9, France*
[9]*Grand Accélérateur National d'Ions Lourds (GANIL), CEA/DRF-CNRS/IN2P3, Bvd Henri Becquerel, 14076 Caen, France*
[10]*LPSC, CNRS/IN2P3, Université Grenoble Alpes, F-38026 Grenoble Cedex, France*
[11]*Department of Physics and Astronomy, The University of Manchester, M13 9PL Manchester, United Kingdom*
[12]*HH-NIPNE, RO-077125 Bucharest-Magurele, Romania*

(Received 4 June 2018; published 31 August 2018)

In this article we report on the observation of new yrast and non-yrast states in ^{136}I, populated in the prompt-γ spectroscopy EXILL campaign at the ILL using both ^{235}U(n,f) and ^{241}Pu(n,f) reactions. We propose an extension of the level scheme and interpretation of the new spectroscopic results in comparison to state-of-the-art shell-model calculations. We discuss the role of the proton $d_{5/2}$ orbital in the structure of this nucleus with $Z = 53$ and the energy split between the $\pi d_{5/2}$ and $\pi g_{7/2}$ orbitals. We also provide a complete overview of all experimental information about this nucleus and include new data from ^{252}Cf, ^{248}Cm fission and β decay of ^{136}Te to ^{136}I. We give a new interpretation of ^{136}I and its decay to ^{136}Xe in terms of the influence of the neutron $h_{9/2}$ orbital and the Gamow-Teller strength for $N = 83$.

DOI: 10.1103/PhysRevC.98.024323

I. INTRODUCTION

The doubly magic nucleus ^{132}Sn and few valence particle nuclei around it are neutron-rich species that have been of particular interest for several decades. In addition to the study of the $_{50}$Sn isotopes and their various neutron excitations themselves, the $_{51}$Sb and $_{53}$I isotopes can provide further insight into the different channels of the nucleon-nucleon interaction and, in particular, into the proton-neutron one and the associated coupling schemes, developing in the vicinity of ^{132}Sn. At $Z = 53$, the influence of the three particles, acting as a cluster [1] in the iodines has been used to explain some of the features of these nuclei [2]. It was expected that such three-proton configurations would result in a more complex level structure in the odd-odd I isotopes than in the odd-odd Sb with one valence proton as, for example, ^{132}Sb [3] and ^{134}Sb [4]. Already for ^{134}I, a complicated level scheme and large configuration mixing was reported by the authors of Ref. [5], who needed a three-proton configuration treatment to explain the low-spin states.

The ^{136}I nucleus with one neutron and three proton particles beyond $N = 82$, $Z = 50$ has been studied in earlier works, motivated by its proximity to the double-shell closure and by the presence of both proton and neutron (pn) excitations on the top of the closed ^{132}Sn core. A number of theoretical calculations have also been carried out. Some of them underline the analogy with its isotone ^{138}Cs with $Z = 55$, others—the analogy with the excitations in the next major ^{208}Pb shell, though less evident than for the ^{134,136}Sb nuclei with $Z = 51$ [6]. It is the observation of similarities between ^{137}Cs, ^{135}I and ^{138}Cs, ^{136}I that indicated the importance of the proton excitations around ^{132}Sn [7]. Notably, it is the coupling of the five (or three) protons and the valence neutron that is important in a region with a large neutron excess ($N/Z \sim 1.7$). Moreover, the protons may cause structural changes, or a particular local effect as a function of this neutron excess [8,9], even in the presence of only one of these protons as crossing between the proton $d_{5/2}$ and $g_{7/2}$ orbitals at $N = 89$ [10]. Two other points make this ^{136}I nucleus with $N = 83$ interesting: one is the position of the proton $d_{5/2}$ orbital here and its connection to the spin-orbit strength in neutron-rich nuclei [11], which has been artificially lowered with respect to the $\pi g_{7/2}$ orbital in Ref. [9] to explain the experimental 6^- isomer relative to the 7^- state. Questions about "$j - 1$ anomaly" [12] or

*radomira.lozeva@csnsm.in2p3.fr

"dressed" three-quasi-particle excitation modes [13], could then be raised for such three-valence particle configurations, an effect, discussed for $N = 83$ [14] and $N = 85$ isotones [15]. However, this is related to the apparent lowering of the $5/2^+$ state at $N = 84$ [16], suggested due the development of a neutron skin as a result of rearranging of orbits because of changes in the spin-orbit strength [8]. One has, therefore, an access to verification of these basic effects here. The extra point worth investigating for ^{136}I is the $\nu h_{9/2} \rightarrow \pi h_{11/2}$ Gamow-Teller (GT) strength ($B(GT)$) in the decay of ^{136}Te. This particular transition raises low-spin states at relatively high excitation energy [17] and is especially valuable with respect to the reported quenching of this strength toward the end of the $\nu f_{7/2}$ shell for ^{140}I [18].

In this work we present five different experiments in the study of ^{136}I in particular, performed to make a general study of the structure of neutron-rich nuclei. The (spontaneous, ^{248}Cm and ^{252}Cf, or thermal neutron-induced ^{241}Pu and ^{235}U) fission experiments are used for the population of yrast medium and high-spin states, where different data sets give different advantages, such as high statistics, e.g., ^{241}Pu and ^{252}Cf, higher yield for ^{136}I from ^{248}Cm data, smallest background from complementary channels from ^{235}U. The β-decay data of ^{136}Te to ^{136}I (and to ^{136}Xe) direct or from fission product spectroscopy is another valuable data set populating non-yrast low-spin states with access specifically to high-excitation energies, identified with a good degree of certainty (logft 4.5 to 5), thus providing additional richness and complementarity of these studies.

II. EARLIER STUDIES OF ^{136}I

The ^{136}I nucleus was observed in ^{252}Cf spontaneous fission data [19,20], evaluated by Ref. [21], where several observed levels were reported. Further in this section, we refer to transitions, levels, spin/parities, lifetimes (and their precision when known) as reported in the literature. The ground state spin/parity of ^{136}I was set to (2^-), the first excited state to (2^-) at 87.3 keV and second excited level to (6^-) at 150 keV, found to be a 46.9(1) s [22] isomer with $T_{1/2}$ half that of the ground state (g.s.). Subsequent studies using n-induced fission [23] and the β decay of ^{136}Te [17], reported on several low-lying states and fixed spin/parities, including the g.s. to be 1^-. This was done based on the measured (by the β decay of that state) logft value of 7.5 for the transition to the 0^+ g.s. of ^{136}Xe of first forbidden hindered type. The β-n decay of ^{137}Te was consistent with these conclusions, where several other energies de-exiting the levels at low-spin were observed, although without any spin assignment [24]. For the 738 and 578 keV levels, the authors of Ref. [24] proposed spin/parity of (2^-), while (3^-) for the 222 keV level. All were understood well when assuming $7/2^-$ for the g.s. spin/parity of ^{137}Te.

The first excited state of ^{136}I was measured in Ref. [17] to decay to the g.s. by an $M1$ transition, based on a x-ray detection. Two groups of levels were observed: (1) of low-energy with β feedings of forbidden character (spin/parities 0^- to 3^-), or no-β feedings at all; and (2) of high-energy of allowed character (spin/parities 0^+ to 1^+). Additional spin/parity assignment argumentation were taken from other known $N = 83$ isotones (^{138}Cs, ^{140}La, and ^{142}Pr). Let us note that three states at higher energy (2–3 MeV) were also placed in the level scheme, among which a state of spin/parity 1^+ at 2656.6 keV excitation energy, found to be analogous to the 2026.6 keV state in ^{138}Cs [17].

The low-energy levels of ^{136}I were observed also in an independent β-decay measurement of ^{136}Te, produced in neutron-induced fission of ^{233}U [25]. Similar logft values and argumentation on the spin assignments were given as in Ref. [17]. In addition, the half-lifes of the first excited 2^- and 3^- states were measured to be 60(20) ps and 27(8) ps, decaying by 87.3 and 135.1 keV transitions, respectively. The arguments, following lifetime analysis, β decay, and also total conversion coefficients were consistent with the earlier-proposed $M1$ multipolarities for these decay transitions out of the first and second excited states, for which the authors extracted $B(M1)$ of 0.26(9) W.u. and 0.25(7) W.u., respectively. This places ^{136}I in the class of odd-odd nuclei with $N = 83$ that is characterized by the fastest $M1$ transition rates in the region $A \sim 90$–150 [22], where ^{140}La is the fastest with $B(M1)$ of 0.50(8) W.u.

The yrast states in ^{136}I were first observed in a ^{248}Cm fission experiment with EUROGAM2 and reported in two independent data-analysis works. In the first [26], an yrast band was built on the top of the 7^- state, identified as a long-lived one. States with spin/parity up to 14^+ were placed in the level scheme [26], together with unassigned higher-lying levels, candidates for even-higher spins. The observed level scheme was built based on triple-γ coincidences and compared to shell-model (SM) calculations, tuned on empirical pp interaction energies from ^{134}Te and a pn interaction estimated from the ^{210}Bi level spectrum. In a subsequent work [9], the earlier known long-lived yrast state [21] was identified as the 6^- spin-trap isomer and set at unknown excitation energy (X keV in the expectation range around 200 keV) as no γ decay out of the state was observed. It was connected to the already observed by [26] 7^- state via a transition of 42.6 keV. This low-energy transition was measured using LEPS detectors and its estimated conversion coefficient $\alpha_k = 7(1)$ was consistent with an $M1(+E2)$ multipolarity [9]. The long-lived isomeric state was earlier known to 100% [22] β decay as the g.s. Its position, X, was placed by evaluators at 640(11) keV [27] based on Ref. [28] and later in Ref. [29], based on a Q_β measurement [30]. In Ref. [9], however, a disagreement with literature was discussed (Refs. [15,16] of Ref. [9]), and the isomeric level was placed at about 0.2 MeV above the g.s. due to the unobserved γ branch out of the level. A similar position was proposed already in Ref. [21], where the level was placed at 150 keV. The isomer energy level was measured at 201(26) keV in Ref. [31], in agreement with the expectations of Ref. [9], but its spin was not corrected in Ref. [31]. Intriguingly, the energy splitting between the 1^- g.s. and the 9^- high-spin isomer in ^{212}At is practically the same. There, the analogous multiplet involves $h_{9/2}$ protons coupled to a $g_{9/2}$ neutron because the pn interactions are quite similar in these two multiplets [6,31], but the isomeric spin-trap is for spin $I^{\max} = 9$.

For ^{136}I, the connection of the 6^- isomer to the higher-lying (9^-) to (12^-) states was experimentally established

in Refs. [9,26]. Higher-spin levels beyond (12^-), reported in Ref. [26], were not discussed in Ref. [9]. Instead, the observation of also three non-yrast states was reported at 87.3, 222.2 and 316.7 keV to have spin/parity of 2^-, 3^-, and 4^-, respectively. The first two levels and assignments were already reported earlier in β decay [17].

It is interesting to note that the identification of yrast states in ^{138}Cs [7], the isotone of ^{136}I, from ^{252}Cf fission established similar high-spin level scheme, built on the top of a 6^- isomer. A resemblance also to the positive parity structures observed for ^{136}I can be found for the excitations above the 12^- state in ^{138}Cs [26]. In a more recent work [32], the spin/parities of the 9^- and 11^- states in ^{136}I were established based on angular correlations. The (12^-) state was proposed based on the possible $M1$ multipolarity for the 243 keV transition, de-exciting this level. The authors achieved a good description of their data for $M1$ and $E2$ transitions, with an $M1$ effective operator accounting for the core polarization effects and for the $E2$ with effective charges of 1.55 and 0.7, respectively, for the protons and the neutrons. Spin/parities of the higher-lying states up to 4 MeV were suggested in the works of Ref. [26]. These authors discussed explicitly the assignment of one state decaying by a 1644 keV transition, appeared to be of $E3$ type. They argued that otherwise it would result in a state with a 25-ns lifetime, which was not detected. Around this level three states were suggested also around 3 MeV with given spin suggestions, though these assignments would be consistent with several other possibilities (taking into account that no isomeric state is observed among these states) and that they are of positive parity. We will discuss them in Sec. IV together with all other excited states in ^{136}I.

III. EXPERIMENTAL DETAILS

To study ^{136}I and ^{136}Xe nuclei we used the data from several experiments. Motivations for these measurements and the techniques used are briefly presented below.

A. Measurement of prompt-γ rays from neutron-induced fission of ^{241}Pu

The prompt-γ-spectroscopy measurements were performed in the framework of the EXILL campaigns at the PF1B cold-neutron line, ILL [33]. The detection system composed of 16 HPGe detectors, combining eight Compton-suppressed EXOGAM Clover detectors, 6 Compton-suppressed GASP detectors, and 2 standard (Lohengrin) Clover detectors. A collimated neutron beam with a thermal equivalent flux of about 10^8n/s/cm^2 impinged on a ^{235}U target (99.7% enriched, 575 μg/cm^2 on Zr/Sn backing of about 14 μm) or ^{241}Pu target (78.6% enriched, 300 μg/cm^2, on Be backing of about 25 μm) to produce neutron-rich fission products. The data were collected with a digital acquisition system in a triggerless mode using a 100 MHz clock [33] and analyzed in a multifold coincidence mode, with a 200-ns prompt-time window. Gain shifts, calibrations (using standard ^{152}Eu, ^{133}Ba sources for the low-energy and ^{35}Cl(n,γ) reaction for the high-energy regions) and background subtractions were performed using standard procedures. Further experimental details can be found elsewhere [34].

In the present work we analyzed the prompt data on the neutron-rich iodine nuclei beyond ^{132}Sn, populated up to ^{139}I with very limited statistics. The data allowed us to observe well the ^{136}I nucleus for which we report new spectroscopy information. Lifetime analysis on excited states in the iodines were investigated in the followup EXILL+FATIMA campaign (also using U/Pu targets) [35,36]. In the prompt data on the ^{136}I nucleus we observed γ decays of levels in ^{136}I populated in fission and possibly in β decay. The β-delayed neutron (Pn) channel of the twice weakly produced ^{137}I, is only about 7% [22], therefore, effectively, we consider that no other reaction may be observed to take place. The independent fission yield of ^{136}I is 3.1% in ^{235}U, with a cumulative yield of 5.0% [37]. Thus, 60% of the ^{136}I is populated directly by fission (via yrast of near-yrast cascades) and 40% from β decay of ^{136}Te. For the ^{241}Pu target, the numbers read 3.4% independent, 5.8% cumulative yield, respectively, 41% population from β decay [37]. In some approximation, one would therefore expect in both data sets similar, but not necessarily identical, intensity ratios between transitions seen in fission and in β decay, respectively.

B. Measurement of γ radiation following neutron-induced fission of ^{235}U

The high cumulative yield for ^{136}Te and ^{136}I produced in the fission of ^{235}U+n allowed the determination of angular correlations and directional-polarization correlations in $\gamma\gamma$ cascades of ^{136}I and ^{136}Xe, seen in β decay of ^{136}Te and ^{136}I, respectively. The measurement was performed at the cold-neutron facility, PF1B of the ILL Grenoble. We used the EXILL array [34] comprising, among others, eight large EXOGAM [38] Clover detectors arranged in an octagonal geometry, which enabled precise angular correlation and directional-polarization correlation measurements. For the polarization-sensitivity calibration of the EXOGAM Clovers we used the sensitivity calibration as reported in Refs. [38,39] for the EXOGAM and Eurogam Clover detectors, respectively, and normalized it using the characteristic, known $0^+ \rightarrow 2^+ \rightarrow 0^+$ cascades observed in the EXILL data. For the angular-correlation and directional-polarization analysis we used formulas and conventions of Refs. [40,41] and the technique from Ref. [42].

C. Measurement of prompt-γ rays from spontaneous fission of ^{248}Cm

New medium-spin excitations in ^{136}I were searched for by analyzing triple-γ coincidences between prompt-γ rays from fission fragments populated in the spontaneous fission of ^{248}Cm. The γ radiation was measured using the Eurogam2 array of Anti-Compton Spectrometers [43]. The Eurogam2 array comprised of 6 Low Energy Photon spectrometers (LEPS), with energy resolutions better than 1 keV, which helped when measuring low-energy γ rays and x rays.

In the measurement about 2.5×10^9 high-fold coincidences were collected. The electronic time-coincidence window was 400 ns [44]. Improved analysis techniques developed and

used for the ^{248}Cm fission measurement, provided new information on ^{136}I, as compared to Ref. [9] reporting the same measurement, and compared to Ref. [26] reporting an older measurement of ^{248}Cm fission.

Prompt-γ rays from ^{136}I are analyzed in coincidence with prompt-γ rays from most abundant ^{248}Cm fission-fragment partner ^{109}Tc. To search for new γ lines in ^{136}I and ^{136}Xe we used triple-γ histograms, sorted with various conditions on the time signal. A triple-γ histogram with one axis corresponding to LEPS was used to search for low-energy γ lines and various analyses involving iodine and xenon x-ray lines.

D. Measurement of prompt-γ rays from spontaneous fission of ^{252}Cf

The results from the measurement of ^{241}Pu and ^{248}Cm fission have been verified and extended in a measurement of γ rays following spontaneous fission of ^{252}Cf, performed using the Gammasphere array of Ge detectors at Argonne National Laboratory (see Ref. [45] for details). In the measurement about 1.2×10^{11} triple coincidences were collected, an order of magnitude more than in the measurement of ^{248}Cm fission. The electronic time-coincidence window of 900 ns was about a factor two longer than in the ^{248}Cm fission measurement. Good timing of the ^{252}Cf data provided accurate half-lives in the ns to μs range and an effective use of the delayed coincidences for cleaning γ spectra.

To determine precise angular correlations for γ rays from the discussed ^{252}Cf fission experiment and determine multipolarities of prompt-γ transition in ^{136}I we used the technique of Ref. [46].

E. Measurement of γ rays following β decay of $A = 136$ nuclei produced in neutron-induced fission of ^{235}U

We measured β-delayed γ emission from mass $A = 136$ ions produced in the neutron-induced fission of ^{235}U and selected using the Lohengrin fission-fragment separator [47] equipped with an electrostatic deflector.

The detection setup consisted of an ionization chamber, three Ge detectors (two Clover detectors and a GammaX detector) placed around the chamber. The activity was collected on a stopper foil. The ions were not removed from the measurement point. With a digital acquisition system based on 40 MHz XIA cards we collected triggerless events. In the measurement, which lasted 18 h, with a beam intensity of 1400 ions/s we collected about 3×10^8 triggerless signals from the Ge detectors and the ion chamber. These events were sorted into various double- and triple-γ histograms used to build excitation schemes of ^{136}I and ^{136}Xe (for more details see Ref. [48]).

Because at Lohengrin the ions arrive at the collection point about 1.7 μs after being produced in thermal-neutron-induced fission of an actinide target, inside the ILL reactor, we could observe isomers produced in fission with $T_{1/2}$ from a fraction of a μs up to about 50 μs using the time signal from the ion chamber. We also searched for isomers in the ms range, utilizing the electrostatic deflector of Lohengrin operating at a frequency of 100 Hz with a 5 ms/5 ms beam-on/beam-off cycle.

IV. RESULTS

In this section we present the results obtained for excited levels in ^{136}I and ^{136}Xe from the analysis of data collected in the measurements described above. We use γ-ray energies, excitation energies, spin/parities, and lifetimes either as obtained in the particular measurement, or using the adopted values provided in the respective Tables I and III, further in this section.

A. Excited states in ^{136}I populated in neutron-induced fission of ^{235}U and ^{241}Pu

We observe the ^{136}I nucleus in both target data sets. As with the ^{241}Pu target we accumulated larger statistics, hereafter we present the obtained results. We have independently also examined the ^{235}U target data set for consistency. The strongest (3n) complementary channel is ^{103}Nb (3n) in the ^{241}Pu case and ^{97}Y in the ^{235}U case. Together with the also observed, but weaker, (2n,4n) channels they are very well known [22], allowing an unambiguous assignment of the detected γ-rays.

In the excitation of ^{136}I, at low-energy, three γ transitions are seen in this fission-reaction data. Two of them with energies of 87.0 and 135.0 keV, assigned as the first excited states with spin/parity 2^- and 3^- in β decay [17] were also observed in ^{248}Cm fission [9]. We present a double gate on these 87–135 keV transitions in Fig. 1 with both targets. Before discussing these coincidence relations we would like to note that earlier conversion-electron analysis [9], performed for the transition de-exciting the first excited (87.0 keV) state, resulted in an $M1(+E2)$ character. This was consistent with spin/parity of 2^- for this state and, respectively, 1^- for the g.s. Furthermore, it is in agreement with the earlier evaluations [22] and spin/parity of 3^- for the 222.0 level, as suggested by Ref. [17]. However, the reported conversion coefficient of $\alpha_k = 3.2(8)$ [9] seems too high. For example, pure $M1$ transition results in $\alpha_k = 0.956(14)$ while pure $E2$, in $\alpha_k = 2.88(4)$ [49]. Using gates on two of the strongest transitions (356–2078 keV) on the top the 87–135 keV cascade should result in the same intensities of these transitions (if no parallel branches are present which is the case), after all corrections for efficiency and multipolarity. In performing such a test with this data set, we have found that for the 87.0 keV transition $\alpha_{tot} = 1.8(3)$, corresponding to $\alpha_k = 1.301(19)$ [49] and maximum $M1(+E2)$ mixing $\delta = 0.8(1)$.

In addition to these two transitions seen in both reactions, a third low-energy transition of 94.5 keV was seen on the top of them in the previous fission experiment [9] and placed decaying out of the 316.5-keV state with a suggested spin/parity of 4^-. This transition was not reported in the β decay of ^{136}Te (with 0^+ g.s.) [17], although well in the detection range. This suggests that the 316.5-keV state has spin $I > 3$ and most likely (4^-), on one hand as the 94.5-keV transition is observed rather strongly in Fig. 1 ($E2$ multipolarity will largely decrease its intensity due to conversion in comparison to $M1$),

TABLE I. Energies (E_γ) and intensities (I_γ) in ^{136}I of the observed yrast transitions, as normalized to the strongest 87.0-keV line from ^{235}U/^{241}Pu data and to the strongest 1111.7-keV line from the ^{252}Cf data. The new transitions/levels are marked by (+), the tentative by the (−) symbol. The two (126–159 keV) transitions in the complementary ^{103}Nb are taken as a gate in the ^{241}Pu case. For the relative intensities of all observed transitions multiple gates are used (see text). Best adopted values are also provided. Level excitation energies [E_{exc}(keV)] and uncertainties for our measurements are calculated with respect to the measured energy of the 6$^-$ band-head from Ref. [31].

γ-ray ^{235}U/^{241}Pu data E_γ(keV)	γ-ray I_γ(%)	Level E_{exc}(keV)	γ-ray ^{252}Cf data E_γ(keV)	γ-ray I_γ(%)	Level E_{exc}(keV)	γ-ray Adopted E_γ(keV)	Level Adopted E_{exc}(keV)
42.0(1)	41(3)	243.0(1)	42.8(1)	20(8)	243.8(1)	42.4(1)	243.4(1)
61.3(1)$^+$	0.5(0.3)	3319.8(5)	61.2(1)	8(2)	3324.3(4)	61.3(1)$^+$	3321.4(4)
87.0(1)	100(1)	87.0(1)	87.5(1)	50(7)	87.5(1)	87.3(1)	87.3(1)
94.5(1)	18(2)	316.5(1)	94.7(1)	12(3)	317.3(1)	94.6(1)	316.9(1)
117.2(1)	1.0(0.7)	3258.5(3)	117.5(2)	2(1)	3261.1(5)	117.4(2)	3260.1(6)
135.0(1)	36(3)	222.0(1)	135.2(1)	35(5)	222.6(1)	135.1(1)	222.3(1)
			146.5(1)$^+$	1.5(5)	1761.9(3)	146.5(1)$^+$	1761.9(3)$^+$
			179.5(1)$^+$	4(1)	1795.8(3)	179.5(1)$^+$	1794.9(4)$^+$
181.8(3)	1.0(0.5)	3258.5(3)	182.5(2)	2.5(5)	3261.1(5)	181.8(4)	3260.1(6)
242.9(2)	7(2)	1857.6(3)	243.0(1)	35(5)	1859.5(2)	242.9(2)	1858.3(3)
243.0(5)	0.4(0.1)	3319.8(5)	243.2(1)	10(5)	3324.3(4)	243.1(5)	3321.4(4)
260.7(1)	21(2)	1614.7(3)	260.8(1)	74(3)	1616.3(2)	260.8(1)	1615.4(3)
			407.3(1)$^-$	5(1)	1761.9(3)	407.3(1)$^-$	1761.9(3)
			457.8(3)$^+$	0.5(2)	3142.7(4)	457.8(1)$^+$	3142.7(4)
1039.3(3)$^+$	1.0(0.4)	5357.1(5)	1039.3(2)$^+$	2.5(4)	5357.7(3)	1039.3(4)$^+$	5357.7(6)
1058.3(3)	1.4(0.3)	4316.8(4)	1058.2(1)	3.2(6)	4319.5(2)	1058.3(3)	4318.4(4)
1069.0(3)	1.4(0.2)	2683.7(4)	1070.2(1)	2.8(5)	2686.5(2)	1069.5(3)	2684.9(4)
1111.0(3)	37(2)	1354.0(3)	1111.7(1)	100(3)	1355.5(1)	1111.2(3)	1354.6(3)
1283.7(3)	1.6(0.2)	3141.3(3)	1284.6(1)	4.1(6)	3144.1(3)	1284.4(3)	3142.7(4)
			1527.7(5)$^-$	0.4(2)	3144.1(3)	1527.7(1)$^-$	3142.7(4)
1401.0(3)	1.8(0.3)	3258.5(3)	1401.9(2)	3.3(6)	3261.1(5)	1401.8(4)	3260.1(6)
1461.9(5)	2.2(0.2)	3077.7(4)	1462.9(2)	8(1)	3079.3(3)	1462.9(5)	3078.3(4)
1463.1(4)$^+$	0.8(0.2)	3319.8(5)	1463.0(2)	6(1)	3324.3(4)	1463.1(4)$^+$	3221.4(5)
1643.9(3)	5(1)	3258.5(3)	1644.8(1)	12(1)	3261.1(5)	1644.7(3)	3260.1(6)
1784.0(5)$^-$	⩽0.5	2101.0(5)				1784.0(5)$^-$	2101.0(5)$^-$
			2097.6(2)$^-$	0.7(2)	5357.7(3)	2097.6(2)$^-$	5357.7(3)$^+$

and on the other, as no positive/parity states are observed at low-energy (involving positive-parity orbitals; see Sec. VI). Our assignment would be in agreement with the suggestions of Ref. [9], where $\Delta I = 1$ was proposed. It is important to stress that this transition can be seen in the gate of the complementary ^{103}Nb fragment which supports the earlier conclusions.

In the coincidence spectrum shown in Fig. 1, we identify a new tentative transition with an energy of 1784.0 keV, which

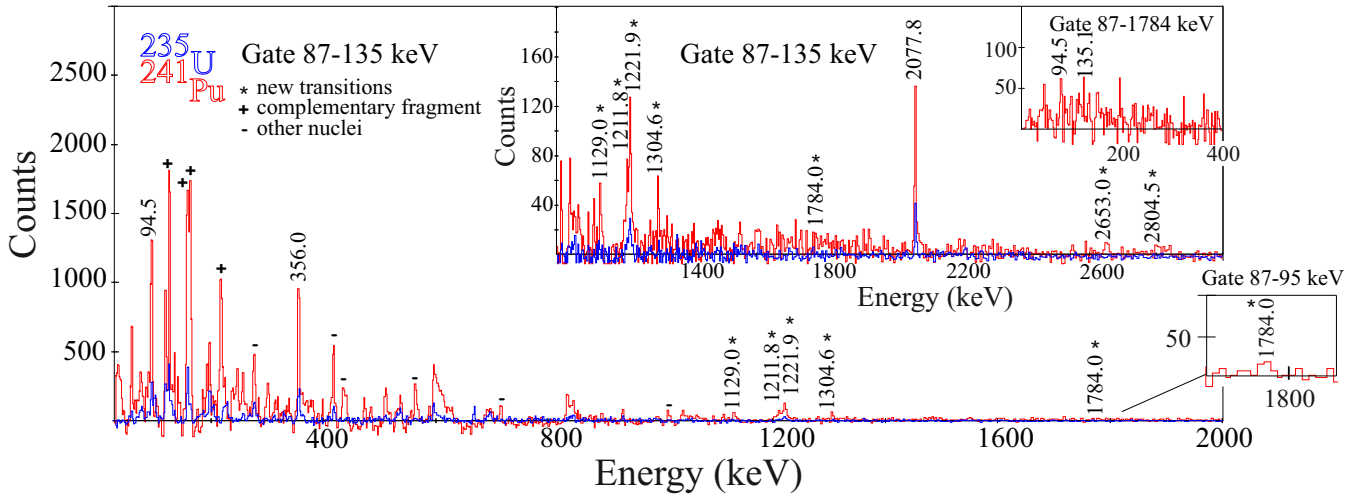

FIG. 1. Coincidence spectra for ^{136}I from neutron-induced fission of ^{241}Pu (red) and ^{235}U (blue) with gates on 87–135 keV transitions with a zoom in the large inset and on 87–1784 keV in the small inset, as measured at EXILL. The new transitions are marked by asterisk (*) symbol.

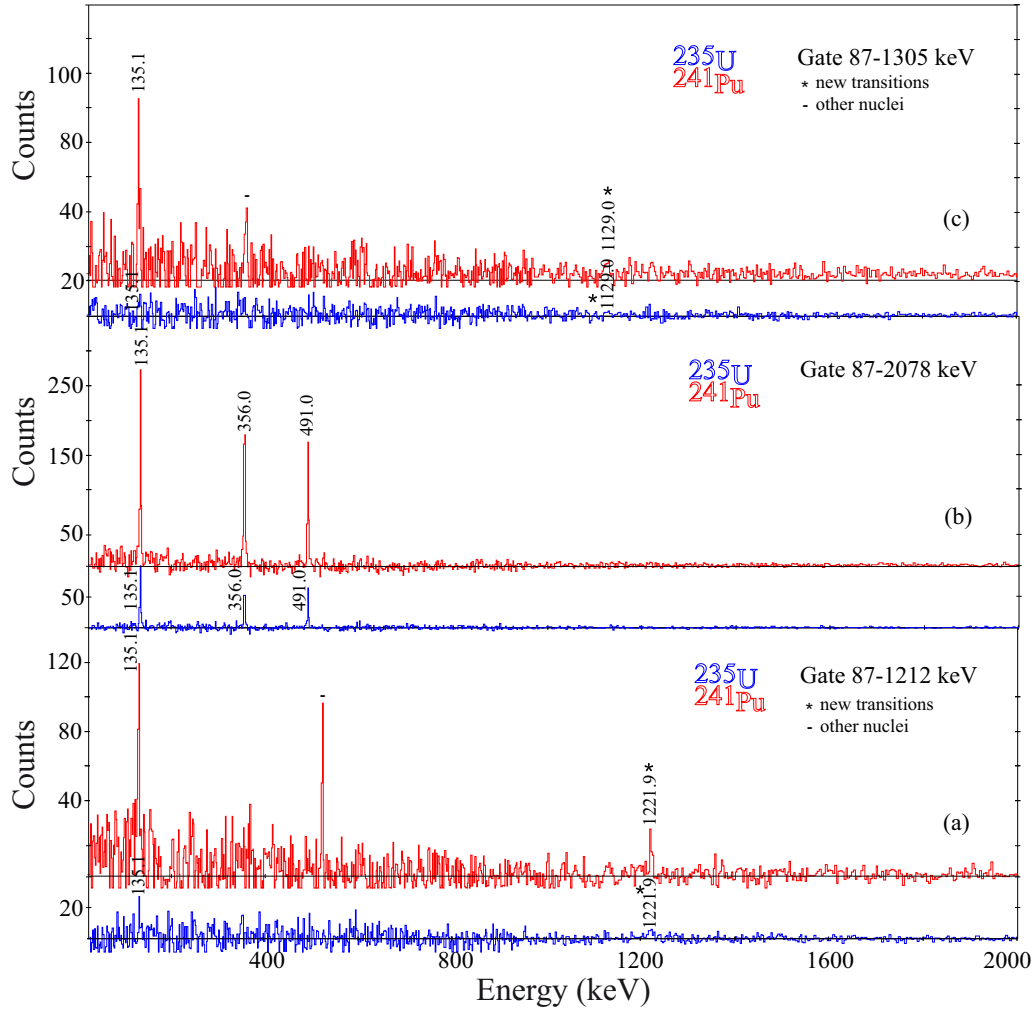

FIG. 2. Coincidence spectra for ^{136}I from neutron-induced fission of ^{241}Pu (red) and ^{235}U (blue) with gates on (a) 87–1212 keV, (b) 87–2078 keV, and (c) 87–1305 keV transitions, as measured at EXILL. The new transitions are marked by asterisk (*).

is in addition in coincidence with the 94.5-keV line (see inset). As this transition is rather weak, we present in addition its gated spectrum 87–1784 keV in the second inset of Fig. 1. This supports the fact that it feeds the 316.5-keV (4^-) state from the fission reaction and most probably also has an yrast origin (see Sec. VI). The new information indicates that these transitions are yrast branches, independent of the yrast excitations built on the 6^- band-head (Sec. IV A 2).

1. Non-yrast states in the level scheme

The known 356.0-keV transition from the β-decay work of Ref. [17], de-exciting a second 2^- state is also observed in our data as it can be seen in Fig. 1 but not in coincidence with the complementary fragment. We have to stress that in our case its intensity is rather strong in comparison to the 11% reported in β^- decay [17] (12% in Ref. [25]), which suggests an alternative population. Some difference in the intensities of other detected transitions supports this possibility (see Sec. IV A 2). It is useful to examine pure β^--decay data to verify the earlier findings.

Several other new transitions with energies of 1129.1, 1211.8, 1221.9, and 1304.6 keV are also observed in our data and cross-checked in multicoincidence relations to belong to ^{136}I. As can be seen in the inset of Fig. 1 their intensities are not very strong and could have been missed in the earlier β-decay work. At an energy of 2077.8 keV, representing a known decay from a 1^+ state, we have observed a strong transition which compares well to the strong 2077.9 keV transition (intensity 119% known from Ref. [17]). The transitions with energies of 2653.0 and 2803.5 keV are also newly observed in this work. We note that the 2804.0-keV transition reported in Ref. [17] has different coincidence relations, therefore in our opinion, we see another line that corresponds to a transition between two other levels.

Various coincidences between, e.g., the lowest 87.0-keV line and other transitions such as those shown in Fig. 2, allowed us to establish their position in the level scheme. With the exception above, the earlier placement [17] well agrees with our observations. We note that for consistency, we have added to Figs. 2 and 3 spectra from the U-target data set, where as it can be seen, the new γ transitions, although weak, are also present. However, it is important to stress that we have some inconsistency with the intensity ratio between the pure β-decay

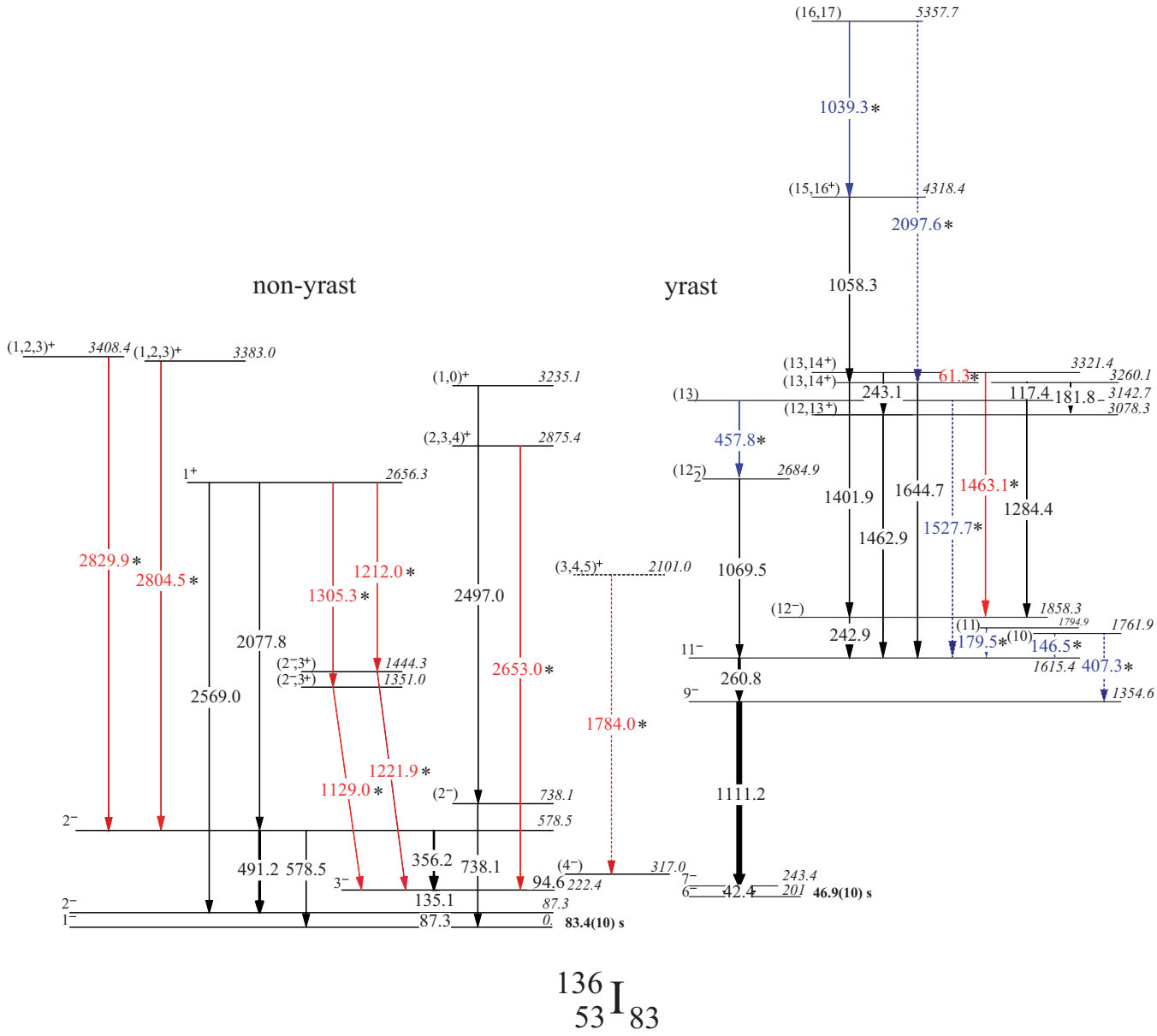

FIG. 3. Experimental level scheme of ^{136}I populated in fission of actinides (yrast) and in β decay of fission products (non-yrast). All new transitions obtained in this work are marked with asterisk (*). The new ones from neutron-induced fission on ^{235}U and ^{241}Pu are in red, the new ones from spontaneous fission of ^{252}Cf fission are in dark blue. The dashed lines represent tentative transitions (levels).

data and our new observations of these non-yrast states. This includes the nonobservation of several transitions such as 630.7 and 3235.1 keV that according to the known β-decay scheme shall be strong (intensities $\geqslant$ 56% [17]). Indeed, we observed well all these transitions in our purely β^--decay work on ^{136}Te $\rightarrow$ ^{136}I (see Sec. IV C). The differences we report may also be due to the different mode of population. This may be true also for the 332.6 keV transition from Ref. [17]. However, no strong coincidence branch has been seen for this transition in the β-decay data to be used as a gate. A line with similar energy (333.9 keV) is also present in the neighboring ^{137}I; therefore, the nonobservation here is inconclusive. The possible spins of the non-yrast levels are further discussed in Sec. VI.

The extended experimental level scheme of ^{136}I is presented in Fig. 3. Its left-part corresponds to non-yrast states, which will be discussed hereafter, with the exception of the branch 1784.0, 94.5, 135.0, 87.0 keV, which is a part of an yrast sequence. In black, we present the already known (from earlier data) transitions, while with an asterisk we indicate those we newly detected in our work (with red or blue colors depending on the data set). The correspondence between detected energies (in the different data sets) and the adopted values used in Fig. 3 are available in Tables I and III. The yrast-part will be discussed in Secs. IV A 2 and IV B.

As proposed earlier, our 2656.3-keV (adopted) level de-excites by the strong 2077.8-keV, 2569.0-keV (adopted)

transitions and the newly observed 1212.0-keV, 1305.3-keV (adopted) transitions. It has a spin/parity of 1^+, which is consistent with our observations and the possible experimental multipolarities. A 3136.8-keV state with $(0, 1)^+$ also reported in β decay to de-excite by a 2804.0-keV transition [17] is most-probably different from the one we detect at an excitation (adopted) energy of 3383.0 keV also de-exciting by a 2804.5-keV (adopted) transition and placed on the top of the 578.5-keV (adopted) level. Moreover, in our data we do not find the branch of a strong 332.6-keV transition reported in cascade with 2804.0 keV in Ref. [17]. Although both higher-lying states seem to have the same parity, we cannot put further constrains on the assigned spin based on the observations from this data set. Interestingly, we have detected other transitions (reported in Ref. [17]) with (adopted) energies of 2497.0 and 738.1 keV to de-excite in cascade another state at 3235.1 keV. One has to note that this state has been set as a 1^+ state in Ref. [22] based on the $(0, 1)^+$ suggestion of Ref. [17] without any measurement on the multipolarity of the de-exiting transitions, therefore we adopt the later assignment. As seen only in single-gate spectra, their intensities are not reported in Table I, together with the rest of the detected transitions.

The newly observed γ rays with (adopted) energies of 2653.0, 2804.5, and 2829.9 keV with most-possibly $M1$ character de-excite states with low-spin (as they decay down to the already known 2^- and 3^- states). The statistics for these transitions is insufficient in this data set to measure multipolarities by performing angular correlations and linear polarization measurements. Therefore, taking into account all possible scenarios for their multipolarities, we give several other spin/parities in the level scheme and compare them to shell-model calculations (see Sec. VI). All of the observed non-yrast states have low-spin and possibly three or four 1^+ levels are observed among them. More candidates for such states are presented in Sec. IV C. Here, we need to comment that these and the new non-yrast states at high energy and low spin were possibly populated in the succeeding β decay of the fission product or by a neutron capture. They are completely decoupled from the yrast multiplet, populated purely in fission. Interestingly, such non-yrast states were reported in $^{127}\mathrm{I}(n, \gamma)^{128}\mathrm{I}$ measurements by Refs. [50,51], where high-energy $M1$ and $E2$ transitions were observed to connect states with low spin from (n, γ) capture states with spins of 2^+ or 3^+. In ^{128}I, for example, the observed non-yrast states are based on the $\pi d_{5/2}, g_{7/2}$ coupling with the neutron (below $N = 82$ in this case) $s_{1/2}$ and $d_{3/2}$ orbitals (thus from four-quasiparticle configurations). The authors of Ref. [50] note that configurations having the same spin and parity probably mix with each other. Their interpretation for the higher-lying (2,3) states is thus based on phonon excitations admixed with quasiparticle states. Distinguishing the entrance angular momentum for producing the nucleus, for example, it was shown in Ref. [51] that in (d, p) and (d, t) reactions one can identify states by transferring $l = 0, 2, 5$ to the s, d, h orbitals in ^{128}I, thus populating levels with spin/parities of $(5, 6)^-$, while with (n, γ) reactions one accesses spins of $(2 \text{ to } 4)^-$. Several 1^+ levels were also reported but only in (n, γ) reactions, e.g., of ^{128}I, and identified as members of the $\pi d_{5/2} \nu d_{3/2}$ multiplet. In our case, similar to the earlier studies we used for the assignments the known spin/parities and transition multipolarities and we took into account that: (i) transitions of unknown (or experimentally indistinguishable between $M1$ and $E2$) multipolarity are not of pure $E2$ type or higher multipolarity (i.e., that any pair of levels connected by such transition differs by at most one spin unit); (ii) the principle that in doubly-odd nuclei the number of $M1$ transitions is at least an order of magnitude higher than the number of $E1$ transitions. It is clear that these assignments are partly based on shell-model considerations, e.g., excitation energies and spin of the levels (see Sec. VI). As we fail to observe other transitions between these levels it is reasonable to assume that the spins of the levels are increasing.

2. *Yrast states in the level scheme*

The already known γ rays from yrast-state excitations in ^{136}I are observed in Fig. 4. We have to note that in our data we detected all of the previously known γ rays, despite using the same ^{248}Cm fission reaction, were reported partially by Ref. [26] and partially by Ref. [9]. The level scheme is built adopting the measured excitation energy $X = 201(26)$ keV [31] for the isomeric 6^- band-head (see Sec. II). According to the detected intensity of the known γ rays, the earlier proposed spin/parity assignments are consistent with our observations. For the transitions 1058.3 and 243.0 keV, connecting states with unknown assignments of possible positive parity [26], we conclude that their mutipolarities are either $E2$ or $M1$, thus spin/parity $(15, 16)^+$ and $(13, 14^+)$, respectively, for their originating states at 4316.8 and 3319.8 keV. Furthermore, based on the possible multipolarities of the deexcitation transitions from the 3077.7- and 3141.3-keV states we add new propositions for their spin/parities as (12^+) and (13^+), respectively, using this data set, which is consistent with our findings in the next Sec. IV B. The correspondence of the different data sets to the adopted values, shown in Fig. 3, is given in Table I.

In addition, we have detected a new transition with energy of 61.3 keV, which can be placed in between the already known 3319.8- and 3258.5-keV levels. Its intensity, as observed in Fig. 4, especially (b,c) is rather strong thus, an $M1$ multipolarity would be in a good agreement with the possible spin of the two levels (assigned previously by Ref. [26]). We observe another new 1463.1-keV transition that can be placed in the level scheme out of the 3319.8 keV level. It is seen in the inset of Fig. 4(b) in the 261–243 keV gate as a strong transition. The earlier observation of the 1461.9-keV γ ray, reported by Ref. [26], is another slightly stronger in intensity transition, placed out of the 3077.7 keV level. This can be proven by the fact that in the 1111–1463 keV gate [see inset of Fig. 4(c)], the 242.9-keV line is observed with more than half of the intensity of the 260.7-keV transition. It means that there is another transition feeding this cascade, which turns out to have an energy of 1463.1 keV. The 243.0 keV transition placed in Ref. [26] out of the 3319.8 keV state, is much weaker than the 242.9-keV line out of the 1857.6-keV level. In cross-coincidence gates we have deduced their intensities (see Table I). We note that, while in the second case it is of $M1$

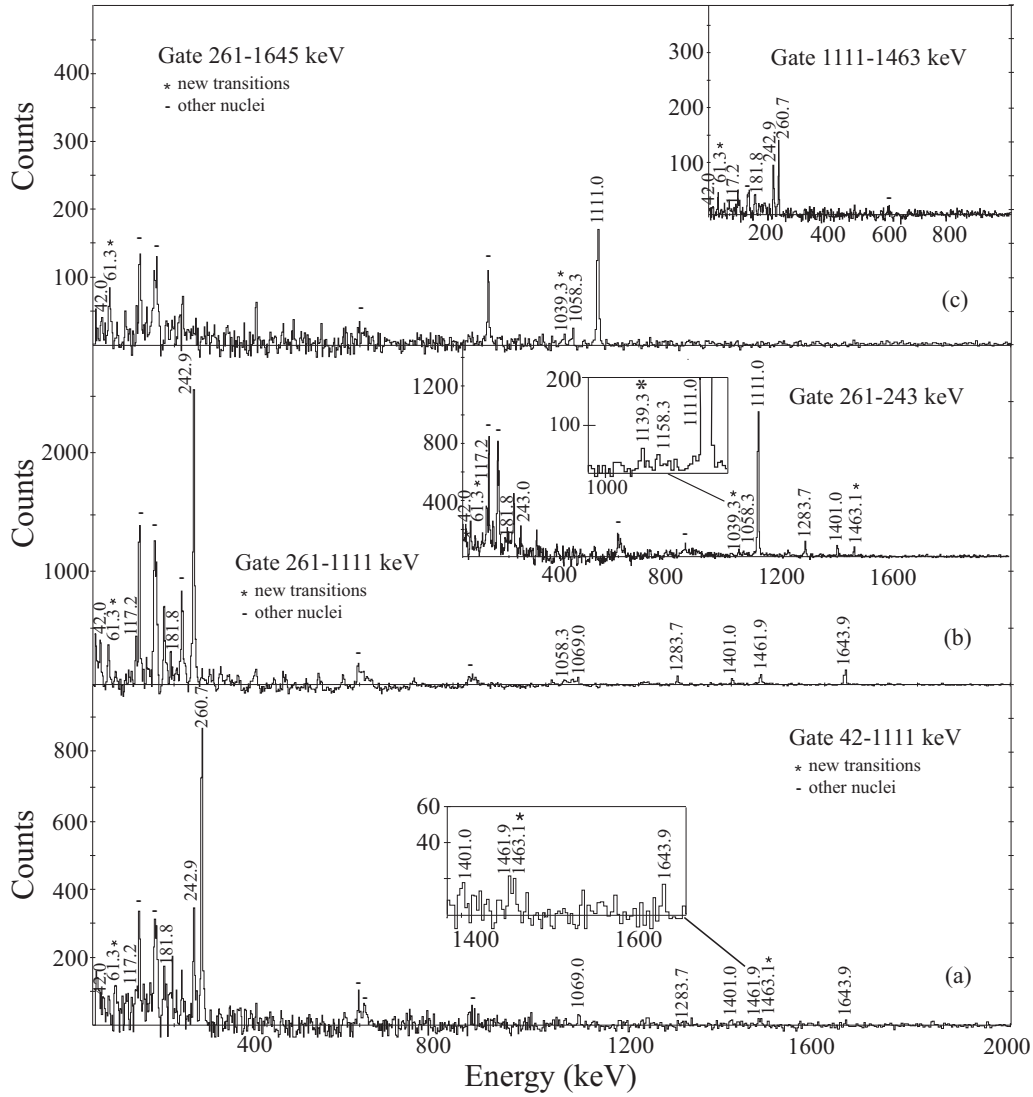

FIG. 4. Experimental spectra for ^{136}I from neutron-induced fission of ^{241}Pu and ^{235}U with gates on (a) 42–1111 keV transitions, (b) 261–1111 keV, and (c) 261–1644 keV transitions, as measured at EXILL. The unidentified peaks belong to the complementary channels/other background. In the insets gates on (b) 261–243 keV and (c) 1111–1463 keV transitions are shown in addition.

character, in the higher-lying case, the 243.0-keV line may also represent an $E2$ decay.

All energies at which we observe the already known and the new transitions in the ^{241}Pu and ^{235}U data sets are listed together with their intensities in Table I. For example, the inconsistency in the energy of the low-spin states mentioned in Ref. [9] is of the order of less than 0.5 keV. Although no intensities were reported in Ref. [26], the strongest line in their level scheme was identified to be 1111.0 keV, reasonably agreeing with Ref. [9]. In our case, we have investigated all γ-ray intensities in multicoincidence gates (e.g., based on the first two band-head transitions noted in Table I) and corrected for efficiency and multipolarity (important for the low-energy ones). All transitions are given with their observed coincidence relations, including the previously known γ rays, confirmed in this work.

A gate on the 243- to 261-keV transitions results in equal intensities for the 1111.0 and the 42.0-keV transitions, which gives certitude of this cascade, as assigned in Ref. [9]. Their intensities of 100% and 10%, respectively, are in variance to our observations taking into account that the 42.0-keV transition is assigned as $M1$ with ($\alpha = 9.2(13)$ [49]). The intensity of the 42.0-keV transition we detect is much stronger than that of the 1111.0-keV transition in both complementary ^{102}Nb (163-193 keV) and ^{103}Nb (126-159 keV) fragment gates. As we cannot exclude, e.g., a pollution of the 42.0-keV transition from other near-lying energies in this data set, we give its intensity in Table I based on the intensity balance.

B. Excited states in ^{136}I populated in the fission of ^{248}Cm and ^{252}Cf

In the present data set, the 42.8-keV transition in ^{136}I is confirmed, making it present in all of our four prompt fission measurements. Its adopted value of 42.4 keV is given together with the other energy correspondences in Table I. In Fig. 5 we

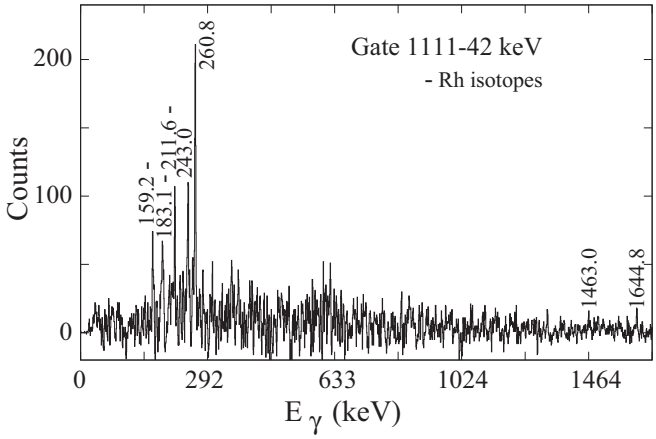

FIG. 5. γ-ray spectrum doubly gated on 1111–42 keV lines of $A = 136$, following the spontaneous fission of ^{252}Cf, as measured at Gammasphere. Strongly nonlinear energy calibration is applied.

show a γ spectrum doubly gated on the 1111.7 and 42.8 keV cascade in the ^{252}Cf fission data, illustrating the data quality. γ lines in ^{136}I above the gating transitions can be seen in the spectrum. The other new low-energy line belonging to ^{136}I, identified at 61.3 keV, is also present in the ^{252}Cf fission data. Figure 6 shows a γ spectrum double-gated on the 1111.7–61 keV cascade, where one can see other transitions of ^{136}I. The present ^{252}Cf fission data allowed to extend even further the high-spin part of the level scheme reported in Ref. [26] and in Sec. IV A 2. In Fig. 7 we show a γ spectrum doubly gated on the 1058.2-keV line and the sum of the 260.8- and 1111.7-keV lines. These and further gates allowed the construction of the yrast excitation scheme of ^{136}I populated directly following fission of actinide nuclei, as shown with adopted transitions and levels and in Fig. 3. The spin/parity assignment to levels in Fig. 3 is based on the same arguments as described in Sec. IV A 2. These include the observed branchings and the assumption that the fission process populates the yrast and near-yrast levels, thus spins are generally growing with the

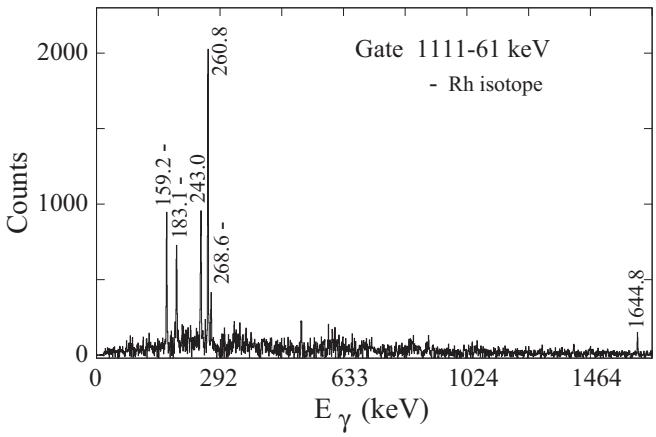

FIG. 6. γ-ray spectrum doubly gated on 1111–61 keV lines of ^{136}I, following the spontaneous fission of ^{252}Cf, as measured at Gammasphere. Energy calibration as in the 1111–42 keV gated spectrum.

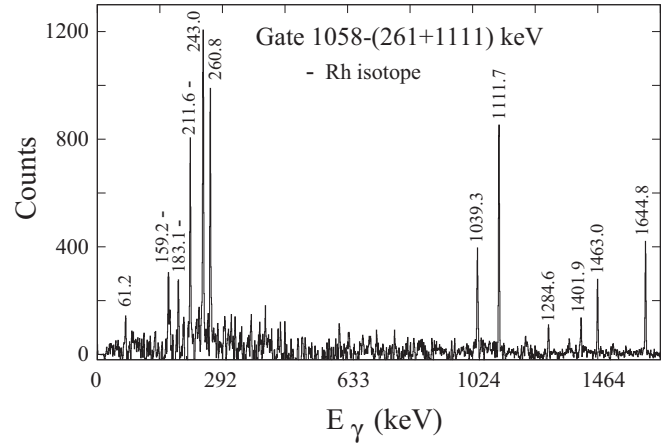

FIG. 7. γ-ray spectrum doubly gated on the 1058-keV line (1st gate) and the sum of the 261- to 1111-keV lines (2nd gate) of ^{136}I, following the spontaneous fission of ^{252}Cf, as measured at Gammasphere. Energy calibration as in the 1111–42 keV gated spectrum.

increasing excitation energy of levels [52]. In addition, we have taken into account angular correlations, which were possible for the strongest $\gamma\gamma$ cascades in ^{136}I, as observed in ^{252}Cf fission data. The results are shown in Table II.

For some low-energy transitions we also estimated α_k conversion coefficients, by observing the ratio of γ intensity to x-ray intensity and/or $\alpha_{\rm tot}$ conversion coefficients from the intensity balance in cascades. For various fission data the results vary but generally are consistent in indicating the possible multipolarities. From the fission of ^{252}Cf and ^{248}Cm we obtained $\alpha_k(42.8) = 8.6(17)$, $\alpha_k(87.3) = 2.9(8)$, $\alpha_{\rm tot}(42.8) = 15(4)$, and $\alpha_{\rm tot}(87.3) = 2.0(3)$, which are consistent with the conclusions in Sec. IV A. The (adopted) 42.4- and 87.3-keV transitions have both an $M1(+E2)$ multipolarity. The (adopted) 1111.2- and 260.8-keV transitions are stretched quadrupoles. They are observed as prompt transitions with no decay which indicates $E2$ multipolarity. The 243-keV transition is a doublet. For the doublet angular correlations indicate $\Delta I = 1$ character. Considering that the (adopted) 242.9-keV component of the doublet dominates, this component has, most likely, a dipole character. The data allow either $M1(+E2)$ or $E1$ multipolarity. The 1463-keV transitions are most likely

TABLE II. Experimental angular-correlation coefficients, a_k/a_0, and the corresponding mixing ratios, δ, of γ transitions in ^{136}I, seen in the spontaneous fission of ^{252}Cf, determined for various spin hypotheses.

Cascade γ_1–γ_2	a_2/a_0 (exp.)	a_4/a_0 (exp.)	Spins I_1-I_2-I_3	δ_{γ_1}
260.8–1111.7	0.108(8)	0.000(12)	11-9-7	
243.2–260.8	−0.058(10)	−0.003(16)	12-11-9	0.02(2)
1463.0–260.8	0.098(42)	−0.062(60)	13-11-9	
1644.8–1111.7	0.16(5)	0.09(7)	14-11-9	
			13-11-9	−0.2(2)

stretched quadrupole while the (adopted) 1644.7-keV transition could be a stretched octupole or mixed $M2(+E3)$ transition.

C. Excited levels in ^{136}I populated following the β^- decay of ^{136}Te

1. Excitation scheme

In the first β^- decay measurement of ^{136}Te to ^{136}I [17], Schussler *et al.* reported on 9 excited levels and 19 transitions deexciting them. In a subsequent study [25], Aas reported 11 excited states and 27 deexciting transitions, changing the energies and placement of some of transitions reported in Ref. [17]. In the present measurement at the Lohengrin separator, we have observed 23 excited levels and 61 deexciting transitions in ^{136}I, among which are 13 new levels and 37 new transitions. From these in Sec. IV A 1 we reported on 12 excited levels and 16 de-exciting transitions among which 3 new excited levels and 7 new transitions as observed in the non-yrast data after β decay of fission products.

The new lines in ^{136}I were identified by time coincidences with known lines of ^{136}I and with the iodine K_α x-ray line at 28.5 keV. The quality of the experimental data is illustrated in Fig. 8, showing low- (a) and high-energy (b) portions of a singles spectrum measured at Lohengrin. Properties of excited levels in ^{136}I and their γ decays are presented in Table III, together with adopted values, taking into account the data from Sec. IV A. The level scheme of excited states in ^{136}I, populated following the β^- decay of ^{136}Te, is shown in Fig. 10, as adopted from our measurements. In the pure β-decay case, relative γ-decay intensities, I_γ, are normalized to 1000 at the 332.9 keV line. These are proportional to the values reported by Aas [25] and differ for some transitions from values reported by Schussler [17]. We confirm the 332.8-keV level and transition energy proposed in [25], which we observe at 332.9 keV, instead of 333.97(6) keV reported in the compilation [27]. The energy of the transition decaying from the first excited state at 87.3 keV is 87.3(1) keV (adopted), instead of the 86.73(7) keV value reported in Ref. [27]. We also confirm the new placement of the 2804.5-keV (adopted) transition, de-exciting the 3383.0-keV (adopted) level, as observed in Sec. IV A 1, and in agreement with Ref. [25], instead of the 3137.1-keV level [17,27], which does not exist. The 3050.1-keV transition populates the 332.9-keV level. We confirm that the 2656-keV line is a doublet corresponding to the 2656.7-keV transition populating the g.s. and the 2656.3-keV transition populating the 578.8-keV level, adopted at 578.5-keV (see Table III). Figure 9 shows a γ-ray spectrum obtained from a $\gamma\gamma$ histogram by gating on this 578-keV line of ^{136}I.

No new isomeric levels with $T_{1/2}$ in a range from ns to ms were found in ^{136}I or ^{136}Xe nuclei in the present measurement. We note that the data on β^- decay of ^{136}Te from the fission experiments in Secs. IV A 1 and IV B are completely consistent with the results from Lohengrin. Moreover, the high-statistics in the measurements with EXILL and Gammasphere enabled the determination of angular correlations and linear polarization for several strong transitions, as discussed in the next section.

2. Spin/parity assignments

Estimates of populations of levels, calculated assuming 8(2)% population of the g.s. in ^{136}I [27], are shown in Table III with label $P/100$. Based on these data we estimated log ft values for levels in ^{136}I, which are shown in the last column of Table III. These values are consistent with the values reported in Refs. [17,25]. In particular, we note the log ft values for (adopted) levels at 2656.3, 3235.1, 3383.0, and 3456.3 keV, which are close to 5.0, indicating allowed unhindered β transitions from the 0^+ g.s. level of ^{136}Te. This, together with the observed branching ratios allows us to a propose spin/parity of 1^+ for these four levels. Here, our results differ from that reported in Ref. [27], where 1^+ spin/parity assignments were proposed for 9 levels. In addition to the 1^+ spin/parity assignments to the (adopted) levels at 2656.3, 3235.1, 3383.0, and 3456.3-keV, based on the log ft values, we assigned spins and parities to other levels using the data from the EXILL and Gammasphere measurements. In Table IV we show angular-correlation results for strong $\gamma\gamma$ cascades in ^{136}I, seen in the β^- decay of ^{136}Te obtained from the EXILL data.

In Ref. [9] spin $I = 3$ was proposed for the (adopted), 222.4-keV level because this level is populated directly in fission, making lower spin unlikely. Spin higher than 3 is not likely because 87.3- and 135.1-keV (adopted) transitions are expected to be of $\Delta I < 2$ multipolarity because of their low energies. Spin 3 was also proposed in Refs. [17,25] based on other arguments. The data shown in Table IV are consistent with this assignment and show a possible mixing ratio for the 135.1-keV (adopted) transition, when $\delta = 0.1$ is assumed for the 87.3-keV transition (this assumption provides the best fit of theoretical angular correlations to the experimental data and is consistent with Ref. [25]). The correlation for the 2569.4–87.3 keV (adopted to 2569.0 keV) cascade agrees best with proposed spins of 1-2-1 in the cascade (with $\delta = 0.1$ of the 87.3 keV transition). Similarly, the correlation for the 2077.8–578.8 keV (adopted to 578.5 keV) cascade is most consistent with spins 1-2-1 in the cascade (with $\delta = 0.1$ of the 87.3 keV transition). The 2496.0–738.1 keV (adopted to 2497.0 keV) cascade is also most consistent with spins 1-2-1. These results provide an extra support for the spin $I = 1$ assignment to the g.s. of ^{136}I. We also note that the high-energy transitions in the three cascades have dominating $E1$ components. The δ values of the 578.5- and 738.1-keV (adopted) transitions, indicate that both of them have $M1(+E2)$ multipolarity, considering their detection in the prompt time window. The 738.1-keV transition is suggested to be predominantly $E2$.

D. Excited levels in ^{136}Xe populated following the β^- decay of ^{136}I

As seen in Fig. 8 lines of ^{136}Xe dominate in these spectra. Our data confirms the scheme of low-spin excitations of ^{136}Xe populated in the β^- decay of ^{136}I, which was determined in a great detail before [25,27] and we use these energies of levels and γ transitions. We do not present any new level scheme. In this work we concentrated on the determination of spins and parities of excited levels, crucial for the spin/parity assignment to the g.s. of ^{136}I and for tracing possible Gamow-Teller

TABLE III. Levels and their γ decays in ^{136}I, as observed in the β^- decay of ^{136}Te and non-yrast states observed in the decay of ^{235}U fission products. The non-yrast states are normalized to the strongest 356.0 keV line after placing a gate on (87–135 keV) transitions in ^{136}I. The new transitions/levels are marked by (+), the tentative by a (−) symbol. In addition, we provide the adopted values taking into account all different measurements. Note that intensities for some of the strongest transitions are not reported from fission product decay data as they appear only in single-gate spectra (thus are possibly polluted).

Level Pure β-decay I^π	Level data E_{exc}(keV)	γ-decay E_γ(keV)	I_γ	γ-decay Fission product E_γ(keV)	decay data I_γ	γ-decay Adopted E_γ(keV)	Level Adopted E_{exc}(keV)	Level $P/100$	log ft
1^-	0.0					0.0	0.0	8(2)	6.7(2)
2^-	87.3(1)	87.3(1)	620(35)	87.3(1)	gate	87.3(1)	87.3(1)	10(3)	6.6(2)
3^-	222.5(1)	135.2(1)	186(7)	135.1(1)	gate	135.1(2)	222.4(2)	2.5(5)	7.2(1)
0^-	332.9(1)	332.9(1)	1000(35)			332.9(1)	332.9(1)	20(2)	6.2(1)
2^-	578.8(1)	356.3(1)	103(5)	356.0(1)	100(3)	356.2(1)	578.5(2)	3.5(3)	6.9(1)
		491.5(1)	104(5)	491.0(1)	45(3)	491.2(1)			
		578.8(1)	830(30)	578.0(1)	71(3)	578.5(2)			
1^-	630.7(2)	51.9(3)	32(9)			51.9(3)	630.7(2)	16(2)	6.2(1)
		297.8(1)	50(7)			297.8(1)			
		543.4(1)	130(8)			543.4(1)			
		630.7(1)	450(15)			630.7(1)			
(3^-)	641.1(3)$^-$	418.7(2)$^-$	12(3)			418.7(2)$^-$	641.1(3)$^-$	0.3(1)	7.9(2)
2^-	738.1(1)	650.8(2)	5(2)			650.8(2)	738.1(1)	1.6(2)	7.2(1)
		738.1(2)	240(10)	738.0(2)	in single gate	738.1(2)	738.1(1)		
(3^-)	988.7(2)$^-$	410.2(2)$^-$	20(3)			410.2(2)$^-$	988.7(2)$^-$	0.4(2)	7.7(2)
		766.3(3)$^-$	7(2)			766.3(3)$^-$			
		901.4(3)$^-$	4(2)			901.4(3)$^-$			
(2^-)	1155.3(2)	932.6(3)	20(5)			932.6(3)	1155.3(2)	0.7(3)	7.3(2)
		1068.0(1)	28(3)			1068.0(1)			
$(2^-, 3^+)$	1351.0(2)	362.3(3)$^-$	16(2)			362.3(3)$^-$	1351.0(2)	−0.1(2)	
		612.8(2)	12(2)			612.8(2)			
				1128.6(1)$^+$	16(3)	1128.6(1)$^+$			
		1350.9(2)	10(2)			1350.9(2)			
$(2^-, 3^+)$	1444.4(2)	813.7(3)$^-$	18(3)			813.7(3)$^-$	1444.3(2)	0.4(2)	7.4(2)
		865.8(2)	4(2)			865.8(2)			
		1221.9(2)	10(2)	1221.9(1)$^+$	24(3)	1221.9(2)$^+$			
		1357.0(4)	5(2)			1357.0(4)			
(1,2)	1972.2(2)	1341.5(2)	18(3)			1341.5(2)	1972.2(2)	0.5(2)	7.1(2)
(1,2)	2145.5(2)	1567.0(2)	22(3)			1567.0(2)	2145.5(2)	0.5(2)	7.0(2)
1^+	2656.7(2)	1212.1(2)	20(2)	1211.8(1)$^+$	20(3)	1212.0(2)$^+$	2656.3(4)	21(2)	5.0(1)
		1305.8(1)	50(4)	1304.6(1)$^+$	18(3)	1305.3(1)$^+$			
		1918.2(4)	40(4)			1918.2(4)			
		2025.7(3)	25(3)			2025.7(3)			
		2077.8(1)	430(15)	2077.7(1)	65(4)	2077.8(1)			
		2323.4(5)	42(4)			2323.4(5)			
		2569.3(1)	290(10)	2568.7(1)	28(3)	2569.0(1)			
		2656.7(2)	25(5)			2656.7(2)			
(1,2)	2724.3(3)	1986.0(2)	5(2)			1986.0(2)	2724.3(3)	0.4(2)	6.7(2)
		2145.7(2)	10(2)			2145.7(2)			
		2636.9(3)$^-$	4(2)			2636.9(3)$^-$			
(1,2)	2863.0(5)	2232.8(5)$^-$	5(2)			2232.8(5)$^-$	2863.0(5)	0.8(2)	6.2(1)
		2284.1(4)	12(2)			2284.1(4)			
		2775.7(2)	22(2)			2775.7(2)			
(1,2)	2868.7(4)$^-$	2290.2(4)$^-$	8(3)			2290.2(4)$^-$	2868.7(4)$^-$	0.2(1)	6.8(2)
(1,2)	2871.6(4)$^+$	2292.9(3)$^-$	12(3)			2292.9(3)$^-$	2871.6(4)	0.3(2)	6.6(2)
		2784.3(2)	6(2)			2784.3(2)			
$(2, 3, 4)^+$				2653.0(1)$^+$	18(5)	2653.0(1)$^+$	2875.4(2)$^+$		
(1,2)	2941.2(3)$^+$	2853.9(2)$^+$	9(2)			2853.9(2)	2941.2(3)	0.2(1)	6.8(2)
(1,2)	3001.4(3)$^+$	2263.3(3)$^-$	7(2)			2263.3(3)$^-$	3001.4(3)$^+$	0.5(2)	6.3(2)
		2914.1(1)$^+$	15(3)			2914.1(1)$^+$			

TABLE III. *(Continued.)*

Level Pure β-decay I^π	Level data E_{exc}(keV)	γ-decay E_γ(keV)	I_γ	γ-decay Fission product E_γ(keV)	decay data I_γ	γ-decay Adopted E_γ(keV)	Level Adopted E_{exc}(keV)	Level $P/100$	log ft
1^+	3235.1(2)	2496.0(1)	86(4)	2497.0(1)	in single gate	2497.0(2)	3235.1(3)	6.2(5)	5.0(1)
		2604.5(3)	22(2)			2604.5(3)			
		2656.3(3)	15(3)			2656.3(3)			
		3147.7(3)$^+$	5(2)			3147.7(3)$^+$			
		3235.1(1)	125(5)			3235.1(1)			
1^+	3383.0(3)	2227.7(1)$^+$	20(3)			2227.7(1)$^+$	3383.0(4)$^+$	3.5(5)	5.1(1)
		2644.6(2)$^+$	3(1)			2644.6(2)$^+$			
		2804.0(3)	52(4)	2804.5(2)$^+$	14(4)	2804.5(4)$^+$			
		3050.1(1)	37(3)			3050.1(1)			
		3295.6(2)	23(2)			3295.6(2)			
		3383.0(1)$^+$	20(2)			3383.0(1)$^+$			
(1)	3408.5(3)	2670.1(2)	10(2)			2670.1(2)	3408.4(4)$^+$	0.5(2)	6.0(2)
		2829.8(2)	25(4)	2830.1(2)$^+$	8(4)	2829.9(3)$^+$			
(1^+)	3456.3(4)$^+$	2825.9(3)$^+$	40(4)			2825.9(3)	3456.3(4)	2.5(3)	5.2(2)
		3123.1(3)$^+$	73(4)			3123.1(3)			

transitions in $A = 136$. To obtain precise angular correlations for strong $\gamma\gamma$ cascades in ^{136}Xe, seen in β decay of ^{136}I we used high-statistics data from EXILL (^{235}U+n in this case), using the technique from Refs. [34,42].

Figure 11 shows the angular-correlation analysis for the 1321.1–1313.0 keV cascade in ^{136}Xe, assuming for the 2634.2-keV level spin of (a) $I = 2$, as reported in Ref. [27] or (b) $I = 1$. The ellipses in the upper panels of Figs. 11(a) and 11(b) represent theoretical values of A_2/A_0 and A_4/A_0 coefficients for the assumed spin hypothesis as a function of the mixing ratio, δ_1 of the 1321.1-keV transition, varying from 0 to $\pm\infty$ (red dots) along the two branches of the ellipse. The 1313.0-keV transition is assumed to be an unmixed, stretched quadrupole with $\delta_2 = 0$. The experimental values of a_2/a_0 and a_4/a_0 with their error bars are represented by blue rectangle boxes [in Fig. 11(b) this rectangle is very small and overlaps with a green cross representing a solution for δ]. Lower panels of Figs. 11(a) and 11(b) show plots of the χ^2 function per degree of freedom. The 1-2-0 spin hypothesis for the cascade is clearly preferred by the χ^2 analysis, indicating spin $I = 1$ for the 2634.2-keV level.

In Table V we show angular correlation results obtained for strong $\gamma\gamma$ cascades in ^{136}Xe, seen in β^- decay of both, the ground state and the 6^- isomer in ^{136}I. We assign spin/parity 2^+ for the 2559.9-keV level, instead of 4^+ reported in Ref. [27] (unlikely to be populated with log ft = 7.6 in the decay of the ^{136}I g.s.). Also worth noting is the 0^+ spin/parity of the 2849.4-keV level, reported previously as $2^{(+)}$ [27].

For some strong transitions in ^{136}Xe we measured directional-linear-polarization correlations in $\gamma\gamma$ cascades, using the EXOGAM Clover detectors as Compton polarimeters. The 1313.1 keV, stretched quadrupole decay of the first 2^+ level in ^{136}Xe [27] served as a known, reference transition in a $\gamma\gamma$ cascade. The results of the linear polarization analysis

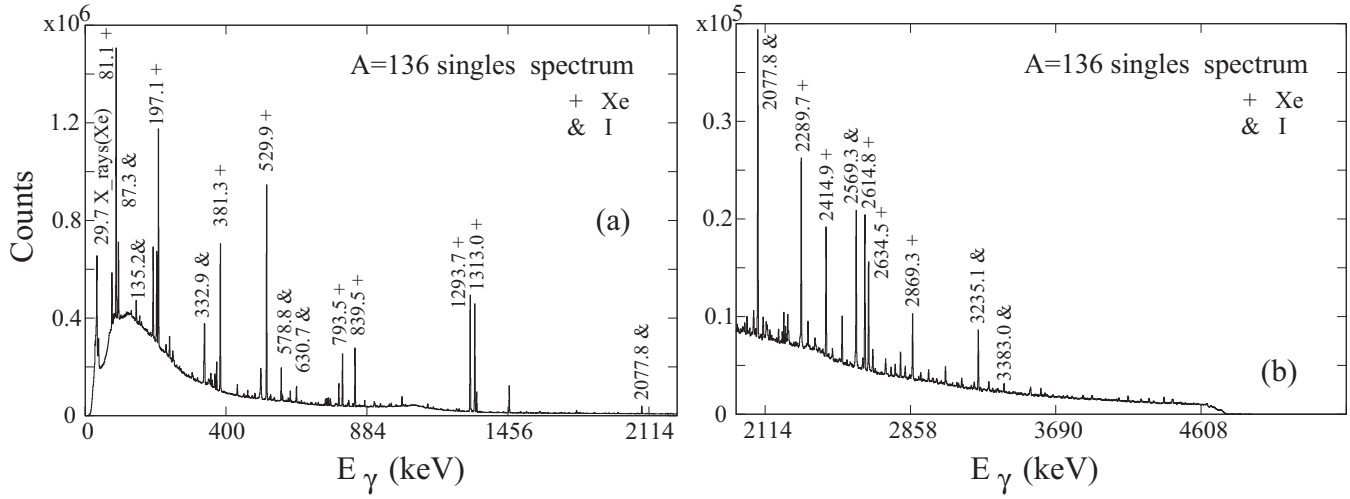

FIG. 8. γ singles spectrum for $A = 136$ nuclei with low (a) and high-energy (b) regions, following β^- decay of ^{136}Te, as measured at Lohengrin. A strongly nonlinear energy calibration is applied.

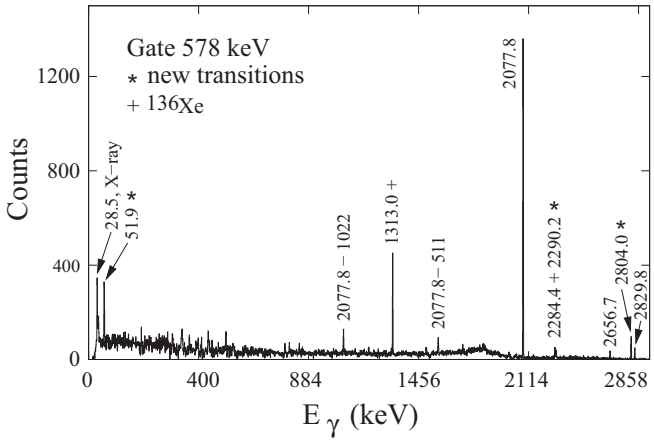

FIG. 9. γ-ray spectrum gated on the 578-keV line of ^{136}I, following β^- decay of ^{136}Te, as measured at Lohengrin. Energy calibration as in the singles spectrum for $A = 136$.

for γ transitions in ^{136}Xe are shown in Table VI in the column $P_{\rm exp}(\gamma^p)$. The last column of Table VI shows theoretical values for linear polarization, $P_{\rm th}(\gamma^p)$, which for a mixed dipole-plus-quadrupole transition can be calculated for the upper transition in a cascade from the formula in Ref. [42]. The values shown in the last column of Table VI were calculated for the polarity shown in the previous column, $M1(+E2)$ or $E1(+M2)$, using a_k/a_0 and δ values for γ_1 from Table V.

Our angular-correlation and linear-polarization data clearly indicates $I^\pi = 1^+$ spin/parity for the 2634.2-keV level in ^{136}Xe. This level has the highest population in the g.s. β^- decay of ^{136}I among all levels populated in ^{136}Xe. A spin/parity of 2^+ was reported for this level in Ref. [27], while a tentative (1^+) assignment was proposed in Ref. [25]. Our data confirms the proposition of Aas *et al.* [25]. The new assignment agrees well with the 1^- g.s. of ^{136}I.

Another important result is the $E1(+M2)$ multipolarity of the 2956.3-keV transition. This results in spin/parity of 2^- for the 4269.3-keV level, reported previously with spin/parity $2^{(+)}$. Our data confirms the $E1(+M2)$ multipolarity of the 1962.2-keV transition [27] and the 3^- spin/parity for the 3275.2-keV level. With the overall population of 2^+ levels lower by about a factor two, as compared to the compilation of [27], the significant population of the 1^+ level and an increased population of 0^+ levels in the g.s. decay of ^{136}I, the argumentation in favour of the 1^- g.s. spin assignment of ^{136}I becomes now more solid.

TABLE IV. Experimental angular-correlation coefficients, a_k/a_0, and the corresponding mixing ratios, δ, of γ transitions in ^{136}I, seen in β^- decay of ^{136}Te, determined for various spin hypotheses. The correspondence to adopted energies is given in Table III.

Cascade $\gamma_1 - \gamma_2$	a_2/a_0 (exp.)	a_4/a_0 (exp.)	Spins I_1, I_2, I_3	$\delta(\gamma_1)$ $\delta(\gamma_2)$
135.2–87.3	0.07(2)	−0.04(5)	$3 \to 2 \to 1$	$\delta(\gamma_1) = -0.4(5)$ or 9(3) $\delta(\gamma_2) = 0.1$
2569.4–87.3	0.23(3)	−0.05(5)	$1 \to 2 \to 1$	$\delta(\gamma_1) = 0.6(2)$ or 1.7(3) $\delta(\gamma_2) = 0.1$
2077.8–578.8	0.12(2)	0.01(4)	$1 \to 2 \to 1$	$\delta(\gamma_1) = 0.7(2)$ $\delta(\gamma_2) = 0.2(1)$
2496.0–738.1	0.27(5)	0.19(12)	$1 \to 2 \to 1$	$\delta(\gamma_1) = 0.8(2)$ $\delta(\gamma_2) = -3.4(5)$

V. DISCUSSIONS

The new data on ^{136}I and ^{136}Xe may help better understanding of two important issues, the strength of β transitions in the $A = 136$ mass chain and the single-particle excitation pattern in this mass region. The former needs to be verified because of recent reports of a significant drop in the $B(GT)$ strength between ^{136}I and ^{140}I [18]. The latter concerns the key question whether the $d_{5/2}$ proton orbital is drastically lowered beyond $N = 82$ due to the formation of a neutron skin, as proposed in Ref. [16], or due another effect causing its crossing with the lowest $g_{7/2}$ proton orbital with the further increase of N [10]. Further, when discussing our results we will refer only to adopted values.

A. Excitations and transitions in ^{136}I and ^{136}Xe

Orbitals active at the Fermi surface in ^{136}I are the $g_{7/2}$ and $d_{5/2}$ protons and the $f_{7/2}$ neutron. Therefore, at low excitation energies one expects two multiplets, $(\pi g_{7/2},\ \nu f_{7/2})_I$ and $(\pi d_{5/2},\ \nu f_{7/2})_I$, with spin I in a range from from 0^- to 7^- and from 1^- to 6^-, respectively. The observation of strong, low-energy, $M1(+E2)$ transitions of 87.3 and 135.1 keV in ^{136}I in both Ref. [25] and this work helps to assign them to low-spin excitations. The $B(M1; 2^- \to 1^-)$ of 0.26(9) W.u. and $B(M1; 3^- \to 2^-)$ of 0.25(7) W.u. [25] indicate that the g.s., the 87.3-keV and the 222.4-keV levels belong to the same $(\pi g_{7/2},\ \nu f_{7/2})_I$ multiplet, the lowest one in excitation energy (see Sec. VI). The intense 578.5-keV and 630.7-keV g.s. transitions are about 50 times slower (with $B(M1) \geqslant 5.9 \times 10^{-3}$ W.u. and $\geqslant 5.6 \times 10^{-3}$ W.u. [25]), which suggests that the 578.5 and 630.7 keV levels belong to the other multiplet. This is clearly supported by the new 51.9-keV transition that we observe to link these two levels, which has an enormous $B(M1)$ of 0.7(2) W.u., which clear supports the fact that ^{136}I possesses some of the highest $B(M1)$ transitions rates in the region.

Higher-energy excitations in ^{136}I are formed when the odd proton is promoted to the $\pi h_{11/2}$ orbital and/or the odd neutron is promoted to the $\nu h_{9/2}$ or $\nu i_{13/2}$ orbitals. For example, the $(\pi h_{11/2}, \nu h_{9/2})_I$ multiplet can be formed with the non-yrast 1^+ member [17], which lies rather high in energy (see Figs. 3 and 10). The other 1^+ and 0^+ states are also based on $[\nu h_{9/2}\pi h_{11/2}(\pi g^2_{7/2})_{0+}]_{1+}$ and $[\nu f_{7/2}\pi h_{11/2}(\pi g^2_{7/2})_{2+}]_{0+,1+...}$ due to the only allowed $\nu h_{9/2} \to \nu h_{11/2}$ transition from the 0^+ g.s. of the mother ^{136}Te (involving both $\nu h^2_{9/2}$ and $\nu f_{7/2}\nu h_{9/2}$ configurations) [17].

This picture is enriched because of seniority $v = 2$ (or $v = 3$) excitations for protons, corresponding to multiplets with spin from $I = 0$ to $I = 18$. As proposed in Ref. [26], the yrast, medium-spin excitations in ^{136}I with spins from 7^- to 14^+ are

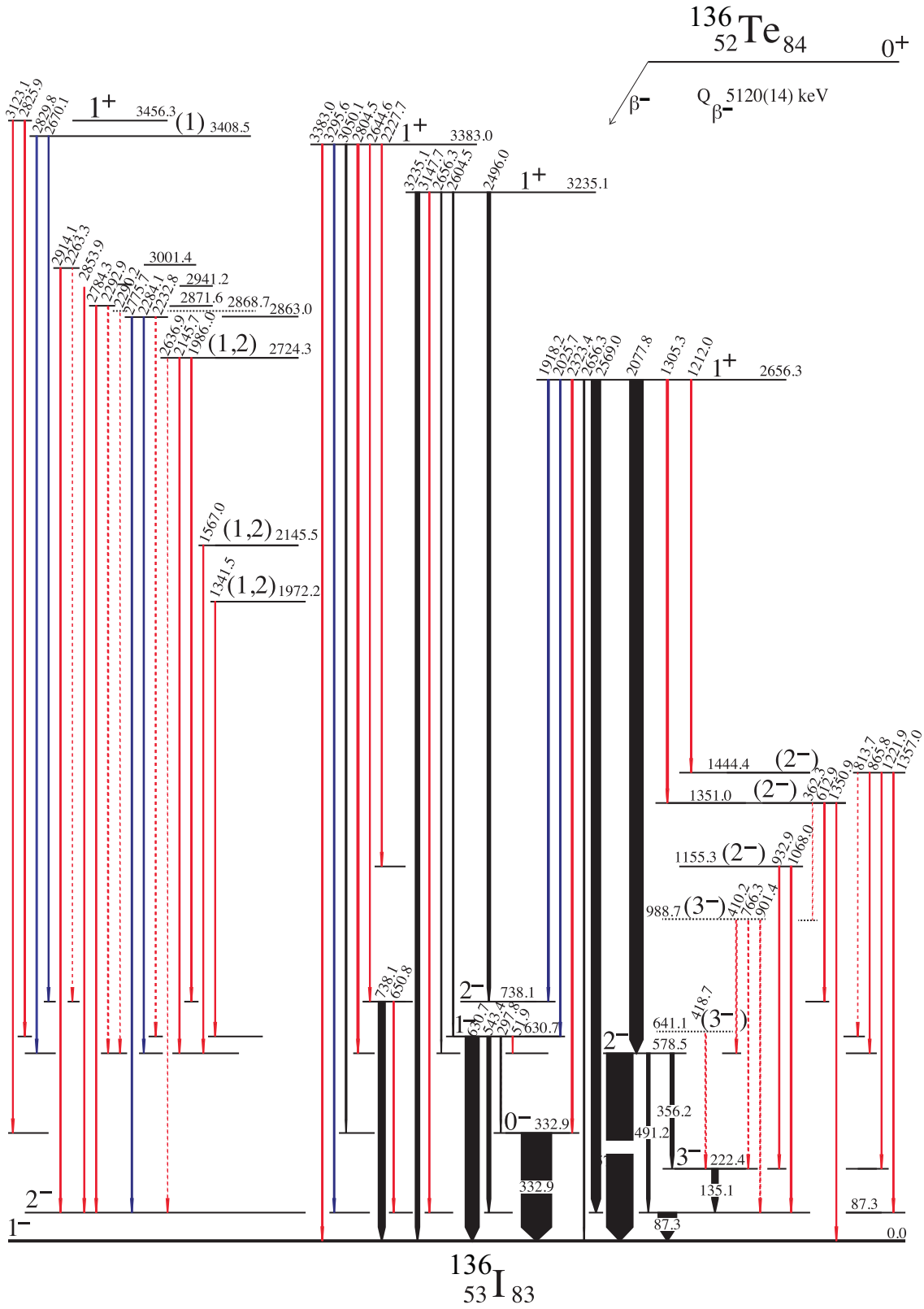

FIG. 10. Level scheme of ^{136}I populated in β^- decay of ^{136}Te, as obtained in the present work. The new transitions are in red, the newly added by Aas *et al.* [25]—in dark blue, and the observed by Schussler *et al.*—in black [17]. The dashed lines represent tentative transitions (levels).

TABLE V. Experimental angular-correlation coefficients, a_k/a_0, and the corresponding mixing ratios, δ, of γ transitions in ^{136}Xe, seen following the β^- decay of ^{136}I, determined for various spin hypotheses.

Cascade $\gamma_1-\gamma_2$	a_2/a_0 (exp.)	a_4/a_0 (exp.)	Spins I_1, I_2, I_3	$\delta(\gamma_1)$
750.1–381.4	−0.435(25)	−0.003(46)	$5\to4\to2$	−0.9(3)
381.4–1313.0	0.103(10)	0.009(23)	$4\to2\to0$	
1246.8–1313.0	−0.160(50)	0.154(101)	$2\to2\to0$	0.62(11)
			$3\to2\to0$	−0.11(7)
			$4\to2\to0$	No solut.
1267.9–1313.0	0.15(35)	1.3(5)	$0\to2\to0$	
1321.1–1313.0	−0.168(13)	−0.011(28)	$1\to2\to0$	−0.08(1)
			$3\to2\to0$	−0.12(2)
			$2\to2\to0$	No solut.
1536.4–1313.0	0.35(10)	1.30(22)	$0\to2\to0$	
			$2\to2\to0$	No solut.
1962.2–1313.0	−0.12(4)	0.03(8)	$3\to2\to0$	−0.07(5)
2956.3–1313.0	0.35(8)	0.10(20)	$2\to2\to0$	−0.16(14)
344.7–2289.6	−0.26(4)	0.01(8)	$1\to2\to0$	0.01(4)
			$2\to2\to0$	No solut.

dominated by members of the $(\pi g^3_{7/2}, \nu f_{7/2})_I$, $(\pi g^3_{7/2}, \nu h_{9/2})_I$, and $(\pi g^2_{7/2} h_{11/2}, \nu f_{7/2})_I$ multiplets. For some of these yrast states such as the 6^- isomer, the $\pi g^2_{7/2} d_{5/2} \nu f_{7/2}$ configuration was also debated in the past [9], at odds with our calculations (see Sec. VI).

For the non-yrast states fed in the β decays of ^{136}Te and ^{136}I one can propose a scenario as sketched in Fig. 12. Here, the GT decay of the $h_{9/2}$ neutron admixture in the g.s. of ^{136}Te, populates preferably the $(\pi h_{11/2}, \nu h_{9/2})_{1^+}$ configuration in ^{136}I. At the same time, the first forbidden (FF) decay of the $g_{7/2}$ neutron, the major component in the g.s. of ^{136}Te, to the $g_{7/2}$ proton, explains pronounced β decays to the g.s. and low-energy states of ^{136}I. It is interesting to note that the excitations and decays in $A = 136$ mass nuclei near the $N = 82$ line resemble the scenario observed in mass $A = 86$ nuclei near the $N = 50$ line [42]. In both cases there are clear GT transitions to 1^+ and 2^- levels in odd-odd and even-even nuclei, respectively, which subsequently decay by intense $E1$ transitions. Pronounced decays of 1^+ levels at 2656.3 and 3383.0 keV to the g.s. and the 1^- and 2^- excited levels

TABLE VI. Experimental, $P_{\rm exp}(\gamma^p)$, and calculated $P_{\rm th}(\gamma^p)$ values of linear polarization for γ^p transitions in ^{136}Xe, seen in β^- decay of ^{136}I, as obtained in the present work.

Cascade $\gamma_1\to\gamma_2$	$P_{\rm exp}(\gamma^p)$	Spins in cascade	Multipol. of γ^p	$P_{\rm th}(\gamma^p)$
1321.1^p–1313.0	−0.50(12)	$1\to2\to0$	M1+E2 $\delta=-0.08$	−0.40(1)
1962.2^p − 1313.0	0.42(20)	$3\to2\to0$	E1+M2 $\delta=-0.07$	0.20(2)
2956.3^p–1313.0	−0.5(3)	$2\to2\to0$	E1+M2 $\delta=-0.16$	−0.38(2)

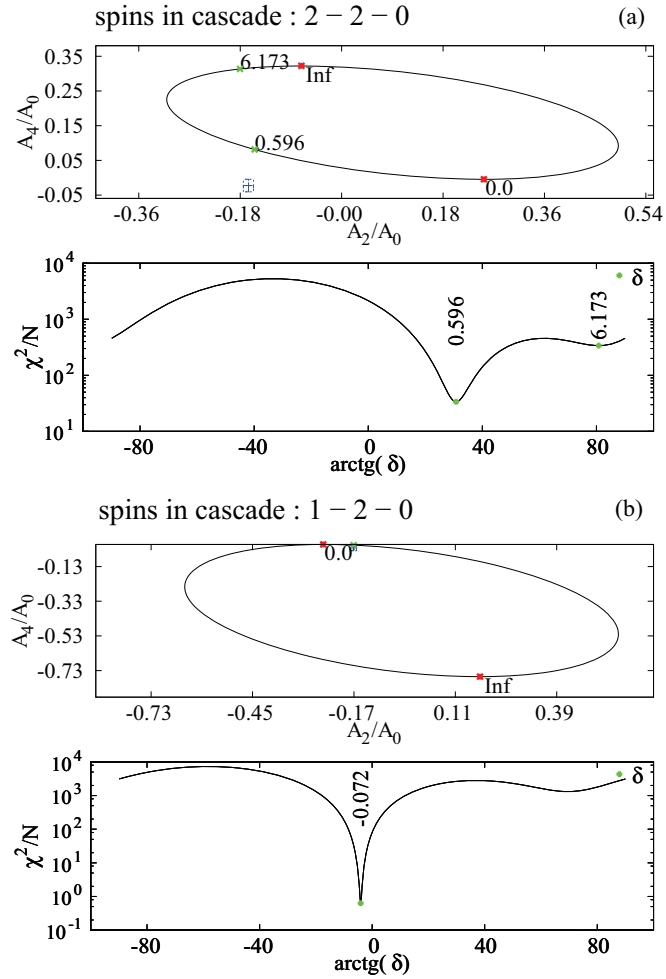

FIG. 11. Angular correlations analysis for the 1321–1313 keV cascade in ^{136}Xe, populated in β^- decay of ^{136}I, for (a) $I = 2$ and (b) $I = 1$ spin for the 2634-keV level.

in ^{136}I could be understood as due to such $E1$ transitions, enhanced by octupole coupling between the $h_{11/2}$ and $d_{5/2}$ or $g_{7/2}$ protons, present in the initial and final states, respectively. Furthermore, as pointed out by Aas *et al.* [25], one observes a strong hindrance of the first-forbidden β transition from the 1^- g.s. of ^{136}I to the 0^+ g.s. of ^{136}Xe (marked with a question mark in Fig. 12). With its log ft ≈ 8.4 [25] this decay is significantly slower than the analogous transition between the ^{134}Sb and the ^{134}Te g.s., for which log ft = 5.2. In the past this difference was associated with the proposed $(\pi g^2_{7/2} d_{5/2}, \nu f_{7/2})_I$ g.s. structure of ^{136}I [53] but this explanation has been challenged in Ref. [25].

VI. SHELL-MODEL CALCULATIONS

To compare the experimental data for ^{136}I and ^{136}Xe nuclei to theoretical predictions, large-scale shell-model calculations are performed using the NATHAN shell-model code [54,55]. They contain the model space $r4h - r5i$, spanned by $1f_{7/2}, 0h_{9/2}, 1f_{5/2}, 2p_{3/2}, 2p_{1/2}, 0i_{13/2}$ orbitals for neutrons and $0g_{7/2}, 1d_{5/2}, 1d_{3/2}, 2s_{1/2}, 0h_{11/2}$ orbitals for pro-

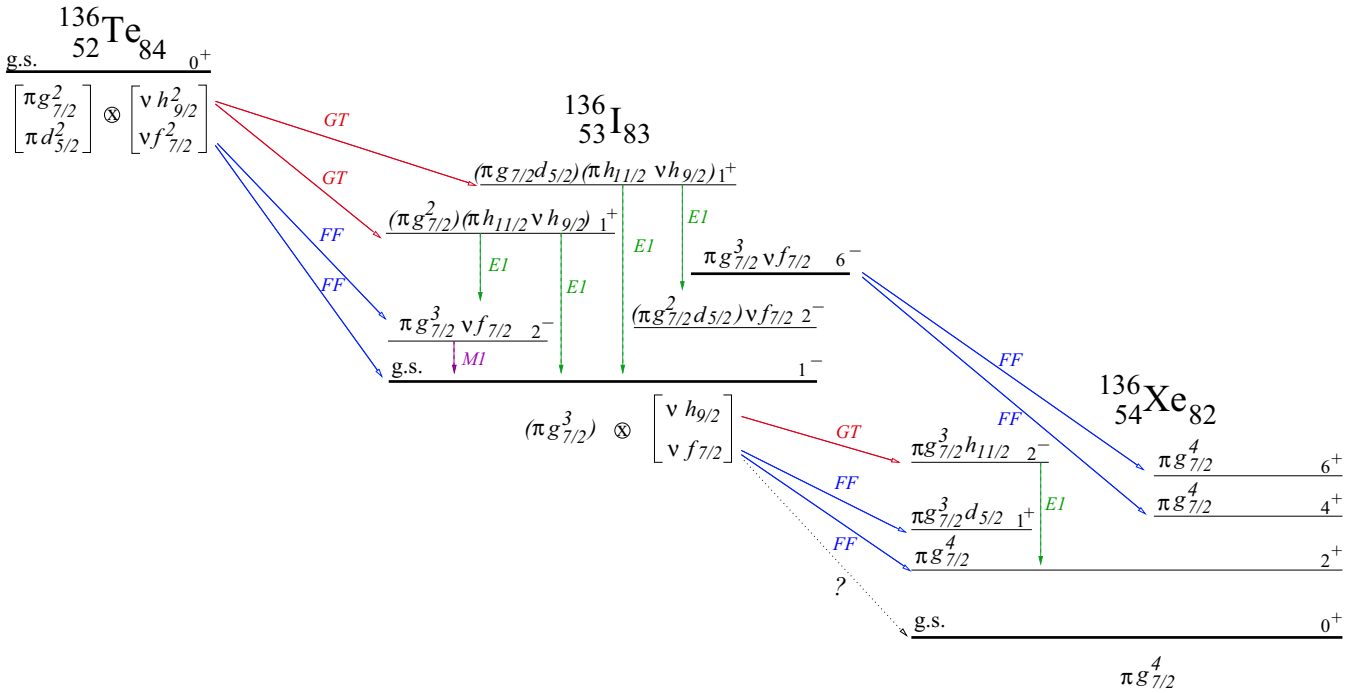

FIG. 12. Schematic drawing of the proposed decay scenario in $A = 136$ isobars, involving the $\nu h_{9/2} \rightarrow \pi h_{11/2}$ GT decay.

tons, above the closed ^{132}Sn core. The corresponding single-particle energies for neutrons and protons are taken from experimental data on ^{133}Sn and ^{133}Sb [22]. The $0i_{13/2}$ neutron and $2s_{1/2}$ proton orbital energies are empirical values taken from Refs. [56] and [57], respectively.

The calculations are carried out using the N3LOP effective interaction, derived from the Chiral effective field theory potentials N3LO [58]. It is adapted to the model space by means of many-body perturbation theory [59], including all the $\hat{Q}$-box folded-diagrams up to the second order. The N3LOP effective interaction was successfully used before in describing the spectroscopic properties and collectivity of even-even chains of nuclei [46] and for odd-even and even-odd mass nuclei [60] around ^{132}Sn.

A. ^{136}I

The results of the present calculations for ^{136}I are shown in Figs. 13 and 14, respectively, where the scale of the observed excitations of 4.5 MeV is reproduced correctly. We note some of the lower-lying states with negative parities ($I = 1 - 5$) correspond to the non-yrast excitations discussed in Sec. IV A 1, with the exception of the first excited $I = 2, 3, 4$ seen in fission. They are well separated from other negative-parity states ($I = 6 - 12$), which represent the yrast excitations discussed in Sec. IV A 2. The higher spins (9 to 16) with positive parity are suggested to connect the highest part of the yrast states in the level scheme. The possible appearance of second excited states with spins between (11^+ and 14^+) is thus also evident. In this nucleus we have in addition rather high excitation energy for the non-yrast states of low spins (0^+ to 4^+) also reasonably well described by the shell-model calculations. Particularly interesting are the different 1^+ states that may have similar origin, as they are reasonably high in energy, their appearance represents an occupation of higher-lying orbitals in their wave functions. We have also a large energy gap for the decay out of one of the new states at 2101.0 keV excitation energy with a most likely (5^+) assignment, as it is part of the yrast sequence. It is, however, drastically different to, e.g., the (3^+, 4^+) states,

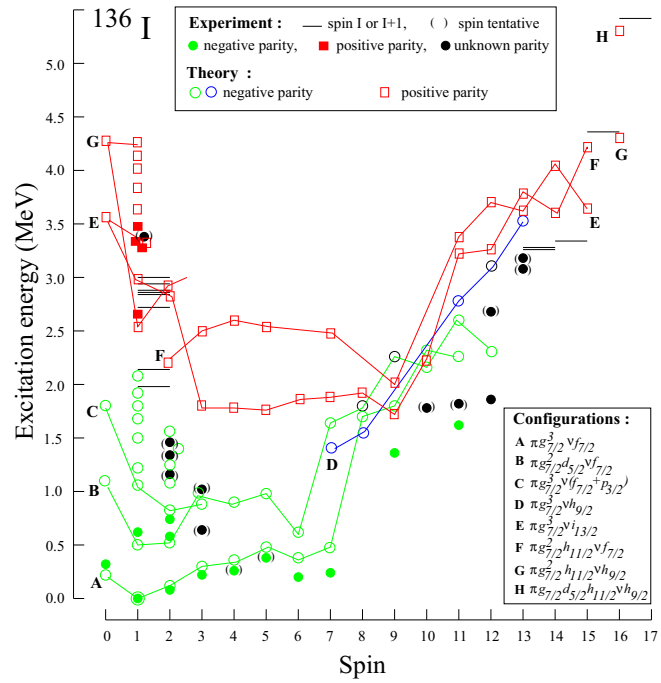

FIG. 13. Comparison of calculated and experimental levels in ^{136}I. Calculations are normalized to experiment at the g.s. level. Dominating configurations are given. See text for more details.

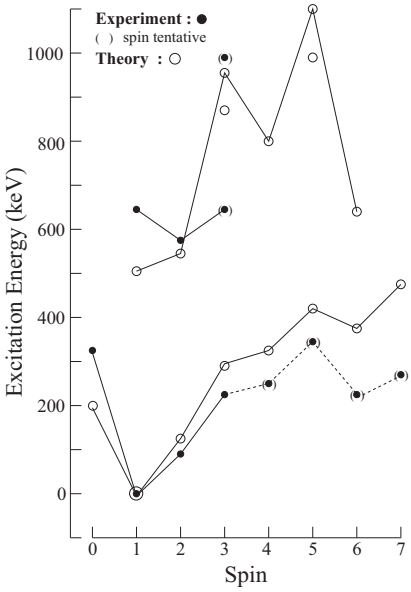

Level	Dominating configurations $\pi g_{7/2}^3 \nu f_{7/2}$ ⊕ $\pi g_{7/2}^2 d_{5/2} \nu f_{7/2}$	$\pi g_{7/2}^2 d_{5/2} \nu f_{7/2}$
0_1^-	80 %	—
0_2^-	43 %	13 %
0_3^-	29 %	49 %
1_1^-	78 %	2 %
1_2^-	3 %	69 %
1_3^-	88 %	1 %
2_1^-	75 %	2 %
2_2^-	4 %	51 %
3_1^-	80 %	2 %
3_2^-	52 %	3 %
3_3^-	9 %	57 %
4_1^-	80 %	1 %
4_2^-	2 %	56 %
5_1^-	81 %	2 %
5_2^-	49 %	3 %
5_3^-	3 %	63 %
6_1^-	82 %	3 %
6_2^-	—	78 %
7_1^-	82 %	—
7_2^-	—	8 %
7_3^-	17 %	69 %

FIG. 14. Comparison of experimental and calculated multiplets in ^{136}I, The "—" symbol in the Table signifies contribution below 1%.

which are also possible based on spin/parity arguments, but with different configurations with a non-yrast origin.

As discussed in the previous section, levels below 500 keV belong to the $(\pi g_{7/2}^3, \nu f_{7/2})_I$ multiplet. These levels are reproduced exceptionally well, as shown in Fig. 14. Among others, the calculations agree well with the existence of a 6^- spin-trap isomer in ^{136}I. In Fig. 14 we propose that the 94.6-keV transition, shown in Fig. 3 between levels with spins 4^- and 3^-, may link the $I = 5^-$ and $I = 4^-$ members of the multiplet, therefore the assignment is tentative.

The dominating $[(\pi g_{7/2}^3, \nu f_{7/2}) + (\pi g_{7/2} d_{5/2}^2, \nu f_{7/2})]$ components in the wave functions of the multiplet members add up to about 80%, as shown in the table in Fig. 14. This indicates a rather simple single-particle (s.p.) structure for all 0^- to 7^- members of the multiplet built on the coupling of the $g_{7/2}^3$ proton and the $f_{7/2}$ neutron. The calculated $B(M1, 2_1^- \rightarrow 1_1^-)$ rates of 1.04 μ_N^2 (0.58 W.u.) and $B(M1, 3_1^- \rightarrow 2_1^-)$ of 0.97 μ_N^2 (0.54 W.u.) compare reasonably well to the experimental values of 0.26(9) W.u. and 0.25(7) W.u., respectively [25].

In Fig. 13 one sees the entire $(\pi g_{7/2}^3, \nu f_{7/2})_{I\max=11}$ structure, labeled "A." Except the 1^- g.s. 2_1^-, 3_1^- members, the yrast 4^- (and 5^-) are candidates for this configuration together with the isomeric 6^-, the 7^-, 9^-, (10), and 11_1^- states.

We note that the calculated 1_1^- g.s. contains only 2% of the $(\pi g_{7/2}^2 d_{5/2}, \nu f_{7/2})$ configuration, thus not supporting the explanation of a hindered decay from this state to the 0^+ g.s. of ^{136}Xe, as proposed in Ref. [53]. This $(\pi g_{7/2}^2 d_{5/2}, \nu f_{7/2})_I$ structure is formed when one proton is promoted to the $\pi d_{5/2}$ orbital and is calculated energetically between 0.5 MeV and 1.0 MeV. The simple $(d_{5/2}, \nu f_{7/2})_I$ coupling produces levels with spins from 1^- to 6^-, with this dominating component of about 60%, as shown in Fig. 14. In Fig. 13 the $(\pi g_{7/2}^2 d_{5/2}, \nu f_{7/2})_I$ multiplet with $I^{\max}$ of 12^-, is labeled "B." According to the shell model, the 578.5, 630.7, 641.1, 1794.9, and 1858.3 keV experimental levels most likely belong to this multiplet. The calculated $B(M1, 2_2^- \rightarrow 1_2^-)$ rate of 1.64 μ_N^2 (0.92 W.u.) agrees with the very large experimental value of 0.7(2) W.u., determined for the new 51.9 keV transition. According to the calculations, the transitions between states with the same neutron configuration is preferred up to spin/parity of 12^-, as it can be seen in Fig. 3, namely, $(12_2^-) \rightarrow 11^-$ and $12^- \rightarrow 11^- \rightarrow 9^- \rightarrow 7^-$. In the proton part, for $I > 10$ the $\pi h_{11/2}$ becomes very important, indicating its higher-lying energy placement. This is in agreement with the analysis done in Ref. [61], who succeeded to describe the experimental first excited and g.s. energies in several $N = 82$ isotones and suggested that $h_{11/2}$ is not in the main configurations of the exited states below 2 MeV for the odd-mass and below 3 MeV for the even-A nuclei. These states were interpreted as $\pi g_{7/2}$ or $\pi d_{5/2} \times 0^+$ of the even $A - 1$ nucleus, in agreement to the measured spectroscopic factors, and indicating realistic mixtures of type $g_{7/2} - d_{5/2}$. We note that configurations of type $(\pi g_{7/2} d_{5/2}^2, \nu f_{7/2})$ have very small amplitudes and are thus omitted in this discussion. It is the 2nd largest configuration in the first 0^- and 1^- states with a 20–30% contribution. In Fig. 13 we show another multiplet, labeled "C," which interferes with "B." The experimental levels 738.1 and 988.7 keV may belong to this multiplet. There are also numerous 1^- and 2^- levels calculated in an energy range up to 2 MeV, which are possible theoretical counterparts to experimental levels above 1 MeV with tentative (1,2) and (2^-) spin/parity assignments. We also note the 12_2^- and 13_1^- calculated levels, belonging to the $(\pi g_{7/2}^3 \nu h_{9/2})_I$ multiplet (labeled "D"), which may account for some of the tentative (12) and (13) experimental levels between 2.5 and 3.3 MeV. The $(\pi g_{7/2} \nu h_{9/2})$ coupling is expected near the yrast line, because this is the first neutron excitation ($\nu h_{9/2}$ is closest to $\nu f_{7/2}$ orbital) in the ^{134}Sb isotone. The $\nu h_{9/2}$ is currently placed at 1.56 MeV in ^{133}Sn [22] and it is brought down in energy in ^{134}Sb due to the strong $(\pi g_{7/2} \nu h_{9/2})$ interaction. According to the calculations, the same $(\pi g_{7/2} \nu h_{9/2})$ configuration gives rise to states with spin/parity of 8^- and the second 7^- in ^{136}I, which are not observed experimentally.

Positive-parity levels appear in calculations only above 1.5 MeV, with the proton excited to the $\pi h_{11/2}$ orbit and/or the neutron excited to the $\nu h_{9/2}$ or $\nu i_{13/2}$ orbitals. The lowest-energy multiplet, labeled "E," corresponds to the $(\pi g_{7/2}^3 \nu i_{13/2})_I$ configuration with $0 < I < 16$. For these first excited states the $\nu i_{13/2}$ orbital is fully occupied with the exception for the 0^+, 1^+, and 2^+ states with the inverse situation, e.g., for the second excited positive parity states. These positive-parity yrast states observed to connect to the negative-parity yrast states (see Fig. 3) were proposed with a $\pi g_{7/2}^2 h_{11/2} \nu f_{7/2}$ configuration and identified up to (14^+) in [26] and up to (15^+) state here. According to the shell model, the 16^+ state appears at about 1.5 MeV energy higher with respect to the multiplet of (11^+ to 15^+) states. This is due to the much stronger $\pi g_{7/2}^2 d_{5/2} \nu i_{13/2}$ contribution for the states up to 15^+ and indeed a possible structural change involving the $\nu h_{9/2}$ orbital for the 16^+ state (with 98% of $\pi g_{7/2}^2 h_{11/2} \nu h_{9/2}$ configuration). The observed energy gap can thus be the $\nu h_{9/2} \rightarrow f_{7/2}$ ($M1$) transition ($16^+ \rightarrow 15^+$), in a better agreement with our experimental data. As discussed in

Sec. IV A 2 based on our observations, we rearranged the earlier proposed spins [26] for these positive-parity states, in accordance with the shell model. In this respect we note that higher-spin negative-parity levels would be expected much higher in energy beyond the positive-parity band. Therefore, one may exclude any other parity-changing transitions. Supposing that it is one of the unidentified transitions from the work of Ref. [26], the transition between (16) and (15) should be faster, thus preferred $M1$ instead of the observed one to the assigned (14^+) state with 1058-keV energy [26]. This supposition is inconsistent with the one observed by us and by [26] the 243.1-keV transition, connecting the unidentified level to a (16^+) state, as such an $M3$ transition should make the (15^+) an isomer, which was scanned and not observed, also in our Pu data. Thus, the unassigned level would not be a (15^+) state. We observe another level from the Cf data that is a candidate for an even higher spin of (16) or (17) with possible positive parity, according to the shell model (see Fig. 13), however, due limited statistics we cannot give further arguments on its assignment.

In ^{134}Sb a $(\pi g_{7/2}\nu i_{13/2})_{I^\pi=10^+}$ configuration is observed [56]. It is therefore possible that the 1761.9-keV level in ^{136}I corresponds to the analogous $(\pi g^3_{7/2}\nu i_{13/2})_{10^+}$ coupling, being the only candidate for such a state. At lower spin, the multiple "E" could explain some of the experimental non-yrast levels between 2.5 and 3.0 MeV, and assigned with spins (1,2).

For the GT transitions, most important are the configurations containing the $(\pi h_{11/2}\nu h_{9/2})$ coupling, which may explain the strongly populated 1^+ experimental levels at 2656.3, 3235.1, 3383.0, and 3456.3 keV. The 1^+ member of multiplet "G," corresponding to the $(\pi g^2_{7/2}h_{11/2}\nu h_{9/2})$ configuration reproduces very well the 1^+ experimental level at 2656.3 keV. Energetically, the reproduction of the other states identified theoretically as 1^+ is reasonable and discussed in detail in Sec. VI C. We also have other positive-parity states with spins $0 < I < 4$. The first such group corresponds to $[(\nu h_{9/2}\pi g^2_{7/2})h_{11/2}]_{1^+_1}$ (and $[(\nu h_{9/2}\pi g^2_{7/2})d_{5/2}]_{2^+_3}$), the second group of $[(\nu f_{7/2}\pi g^2_{7/2})h_{11/2}]_{2^+_1,3^+_2,4^+_2}$ and a third group of $[(\nu i_{13/2}\pi g^3_{7/2})]_{\rm rest}$ configuration of states. Furthermore, our analysis shows that most of these excitations are s.p. ones consistent with most of the structure of ^{136}I. Taking into account that the transitions between these high-energy positive-parity states (of low spin) and the lower-lying negative parity states, we observe basically $\nu i_{13/2} \rightarrow \nu f_{7/2}$ and $\nu h_{9/2} \rightarrow \nu f_{7/2}$ transitions of the order of 2 and 1.2 MeV, respectively. The neutron $13/2^+$ and $9/2^-$ s.p. states in ^{135}Te are, respectively, at 2.1 and 1.25 MeV excitation energy [22], which corresponds to the energy range of our observed transitions. The purely proton excitations $\pi h_{11/2} \rightarrow \nu g_{7/2}$ and $\pi d_{5/2} \rightarrow \nu g_{7/2}$ for the $11/2^+$ and $5/2^+$ states in ^{135}Te have lower energies of, respectively, 1.2 and 0.6 MeV [22], suggesting that the large energy gap for our new excited states in ^{136}I is indeed dominated by the neutron excitation. Interestingly, three of these 1^+ states persist still at the end of the $\nu f_{7/2}$ shell for the very exotic ^{140}I, recently examined in Ref. [18]. Although slightly mixed, they contain similar configurations and have a quenched excitation energy (see Sec. VI C).

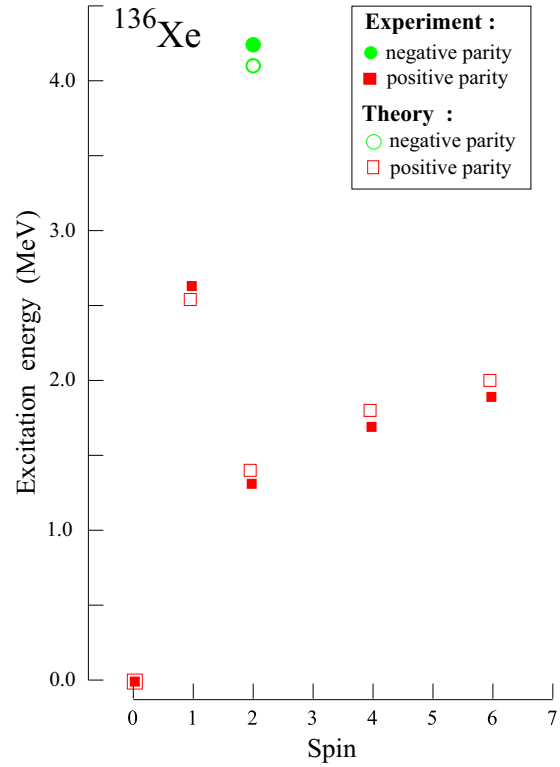

FIG. 15. Comparison of calculated and experimental levels in ^{136}Xe. Calculations are normalized to the experiment at the g.s. level.

B. ^{136}Xe

In Fig. 15 we compare selected experimental levels in ^{136}Xe to their calculated counterparts. The agreement is exceptionally good, validating the choice of s.p. energies and two-body interactions used in our calculations and supporting new results obtained for ^{136}Xe in this work. The experimental levels with spins I of $0^+, 2^+, 4^+$, and 6^+ are reproduced as members of the $(\pi g^4_{7/2})_I$ multiplet, with over 70% content of this configuration in the wave functions of the respective calculated states. For the 0^+ g.s. of ^{136}Xe this contribution amounts to 55%. The mixture of about 23% from the $\pi(g^2_{7/2}d^2_{5/2})_{0^+}$ configuration may influence the g.s. of ^{136}I β-decay rate to this level and may be linked to the measured g.s. to g.s. $logft$ value discussed in Sec. V A.

The prominent, new result shown in Fig. 15 corresponds to the 1^+ level, identified in this work at 2634.2 keV, which was previously assigned spin/parity 2^+ [27]. This experimental level, which receives the highest population in the decay of the 1^- g.s. of ^{136}I, has its theoretical counterpart calculated at 2538 keV with 92% of the $\pi(g^3_{7/2}d_{5/2})$ configuration in the wave function. The theory strongly supports the new 1^+ assignment. The result also suggests that the presence of the $\pi d_{5/2}$ in the coupling is not the reason for low decay rate from the 1^- g.s. of ^{136}I, respectively, invalidating the arguments of Ref. [53]. The 4269.3 keV experimental level in ^{136}Xe, identified in this work as 2^- with log ft = 6.2, is a good candidate for the $\pi(g_{7/2}h_{11/2})$ coupling. This configuration

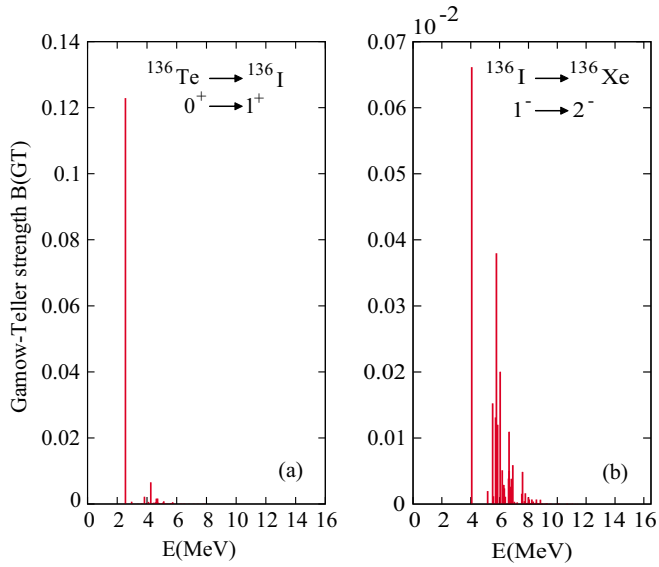

FIG. 16. Calculated Gamow-Teller strength for transitions from ground states of ^{136}Te and ^{136}I to 1^+ and 2^- levels in ^{136}I (a) and ^{136}Xe (b), respectively.

should be populated in GT decay of the 1^- g.s. ^{136}I, containing some admixture of $\nu h_{9/2}$ in its wave function. Indeed, the wave function of the 2^-_1 level, calculated at 4071 keV, contains 78% of the $\pi(g^3_{7/2}h_{11/2})$ configuration, supporting the GT decay scenario shown in Fig. 12.

C. The GT transition strength for $A = 136$

The observed GT decay rates for $A = 136$ suggest that an admixture of a few percent of the $\nu h_{9/2}$ in the wave function of the g.s. of ^{136}Te and ^{136}I might be sufficient to account for them, in analogy to the observed GT rates in the $A = 86$ isobars [42]. The content of the $(\pi g^2_{7/2}\nu h^2_{9/2})$ admixture in the g.s. of ^{136}Te is calculated to be 4%, while the admixture of the $\pi(g^3_{7/2}\nu h_{9/2})$ configuration in the g.s. of ^{136}I is calculated to be 0.9%. These values are lower than the 8% and 1.6% admixture of the $g_{7/2}$ neutron in the g.s. wave functions of, e.g., ^{86}Se and ^{86}Be, respectively [42]. The lower admixture results in slower GT transitions in the $A = 136$ isobars. For 1^+ levels in ^{136}I one observes log ft 5.0, as compared to log ft 4.5 for the analogous 1^+ levels in ^{86}Br [42]. Similarly, for the 2^- level in ^{136}Xe one observes log ft = 6.2, as compared to log ft = 5.3 in ^{86}Kr [42].

We have, therefore, performed the first detailed shell-model study of the GT transition rates for the ^{132}Sn region by investigating the $A = 136$ isobars. The present model space contains different neutrons and protons orbits (see Sec. VI) and the only possible allowed β decay is the transition $\nu h_{9/2} \rightarrow \pi h_{11/2}$. In the first step, we have fixed the renormalization factor to describe the β decay in this restrictive valence space $r4h - r5i$. The mean value of the all renormalization factors which reproduces exactly the experimental log ft values corresponds to 0.55. The B(GT) strength function given in Ref. [54], multiplied by the quenching factor and the sum rule, is plotted in Fig. 16. As can been seen, strong GT transition is obtained from the 0^+ g.s. of ^{136}Te to the first 1^+ state in ^{136}I at 2550.5 keV. This 1^+ state contains about 84% pure $(\pi h_{11/2}\nu h_{9/2})$ configuration, corresponding to log ft value of 4.69 [17,22], which is consistent with the new data of 5.0 (see Table III). Other small GT transitions from 0^+ to 1^+ levels are also identified in Fig. 16(a), with a different $(\pi h_{11/2}\nu h_{9/2})$ coupling in their wave functions at 2968.4 (2%), 3386.9 (2%), 3640.9 (2%), 4071.6 (12%), 4102.2 (39%), and 4255.11 keV (34%). Their amplitudes are still insufficient to get the experimental logft values of 5.0, 5.1, and 5.2 for the 1^+ states, respectively, at excitation energy of 3235.1, 3383.0, and 3456.3 keV.

Regarding the GT transition rates from ^{136}I to ^{136}Xe shown in Fig. 16(b), weak transitions are obtained from the 1^- g.s. to 2^- excited states, with the principal strength corresponding to the 2^-_1 state in ^{136}Xe at 4070.85 keV. The wave function of this state is dominated 78% by the $(\pi g^3_{7/2}h_{11/2})$ configuration, with a log ft value of 6.95, close to the new data of 6.2. In addition, we point out that the calculated strength of GT transitions to 2^- levels in ^{136}Xe is significantly lower than to the 1^+_1 in ^{136}I, in agreement with the experimental log ft values. This reflects the small content of $h_{9/2}$ neutron in the g.s. of ^{136}I as compared to ^{136}Te.

One can correlate the above results to the measurements in ^{140}I with, e.g., log ft of 4.9 for the 1^+_1 level [18], and proposed B(GT) quenching with respect to ^{136}I, resulting in significantly lowered excitation energy of these 1^+ states in ^{140}I. More experimental data is needed in particular for ^{138,142}I to further investigate these conclusions.

D. The $\pi d_{5/2}$–$\pi g_{7/2}$ energy split

A particularly interesting question in the present work is the position of the $d_{5/2}$ proton orbital outside the ^{132}Sn core. It is relative to the position of the proton $g_{7/2}$ orbital that has already been discussed in the Sb isotopes both in the range $58 < N < 82$ in Ref. [11] and beyond $N = 82$ in Ref. [10]. For the first case, it was found that around $N = 70$ the $g_{7/2}$ orbital drops below the $d_{5/2}$ orbital, due to the spin-orbit force (see Fig. 2 in Ref. [11]). The repulsion with the increase of $N > 70$ between these two orbitals has been expected to continue also beyond $N = 82$ and it was a surprise to find the low-lying $5/2^+$ excitations in Sb isotopes with $N > 82$, believed to be the s.p. state (see Fig. 16 in Ref. [16]). To describe their low excitation energy, it was necessary to lower (artificially) the position of the $\pi d_{5/2}$ orbital by a few hundred keV in the shell-model calculations, to describe this experimentally observed drop in ^{135}Sb [16] and believed to be the case in ^{136}I [9]. It was proposed that this lowering occurs due to the formation of a neutron skin [16]. As an even larger adjustment on the energy split between the two orbitals was needed in ^{138}I, the authors of Ref. [62] suggest that the lowering of the $\pi d_{5/2}$ orbital is rather an artefact due some deficiency in the input data used in the shell-model calculations in the ^{132}Sn region, than an effect of appearance of neutron skin, proposed in Ref. [16].

To describe recent experimental data beyond $N = 82$ [10,63], a new development of improved two-body interactions for the region has been performed and such calculations are presented in Ref. [60]. They clearly show a different

behavior of the $\pi d_{5/2}$ orbital with respect to Ref. [9]. In the later referred work, an artificially fast lowering of the $\pi d_{5/2}$ orbital was needed to explain the experimental data on the iodines. Above $N = 82$ the effective $1d_{5/2}$ s.p. energy indeed decreases with the increase of N but slowly, dropping below the $0g_{7/2}$ at $N = 90$. The experimental crossing for antimony nuclei at $N = 89$ [10] is thus theoretically reproduced [60]. The inversion reflects the g.s. of ^{141}Sb, expected to be of spin/parity $5/2^+$ and needs to be verified experimentally.

The mechanism responsible for the lowering of the $\pi d_{5/2}$ with the increase of N is the coupling between s.p. states and the collectivity due to a few valence nucleons, which can be also seen as quadrupole recouping (seniority regime). In the ^{132}Sn region, despite the lower collectivity at $Z = 53$ than in $N = 53$ nuclei outside the ^{78}Ni core, there is a clear analogy between the behavior of effective s.p. energies in both regions. In this sense for example, the "$j - 1$ anomaly" [12], observed at $N = 53$ [14], produces a "collective" $3/2^+$ excitation below the s.p. $5/2^+$ level with $\nu d_{5/2}$ origin. A similarity at $Z = 53$ would be that one observes in even-N nuclei a $5/2^+$ level, which is a "collective" excitation [60], from the $\pi g_{7/2}$ orbital "dressed" in collectivity (in the terminology from Ref. [13]). In a simpler perspective, this is effectively a multiplet member based on the coupling of the $\pi g_{7/2}$ orbital to the 2^+ core of the even-even neighbor, which is energetically lower than the $\pi d_{5/2}$ s.p. state. In odd-odd nuclei at $N = 53$, ^{88}Br and ^{90}Rb, a characteristic $(\nu d^3_{5/2}, \pi f^{-1}_{5/2})_{j,j-1}$ doublet is produced [64]. In this work we identified in ^{136}I at $Z = 53$ an analogous doublet $(\pi g^3_{7/2}, \nu f_{7/2})_{6^-,7^-}$, corresponding to the long-lived 6^- isomer and the 7^- level, lying 42.8 keV above.

The position of $\pi g_{7/2}$ and $\pi d_{5/2}$ has already been discussed in Ref. [17], where configuration mixing between the $[\pi g^3_{7/2}\nu f_{7/2}]$ and the $[\pi d^3_{5/2}\nu f_{7/2}]$ multiplets was suggested to take place. Furthermore, as these states project in the same energy region, this would, e.g., explain the different deexcitation modes from the 2^- level which in ^{136}I goes strongly to the 1^- g.s., while in $N = 83$ isotones feeds preferentially the first 3^- level. In this respect, further studies have been carried out on the crossing between these $\pi g_{7/2}$ and $\pi d_{5/2}$ orbitals also with the proton number, increase between La and Pr [11,17,61].

Going deeper in the comparison of shell model to the experimental data for ^{136}I in terms of the effective occupation of these two orbitals, one notes that for the 2^-_1 state, 62% of the strength is taken by the $\pi g^3_{7/2}\nu f_{7/2}$ configuration with only a 2% admixture from the $\pi g^2_{7/2}d^1_{5/2}\nu f_{7/2}$. For the second excited 2^- state at 578 keV excitation energy, 51% of the wave function is composed from the main $\pi g^2_{7/2}d^1_{5/2}\nu f_{7/2}$ configuration with a 12% admixture from $\pi g^2_{7/2}d^1_{3/2}\nu f_{7/2}$. Including other higher-lying negative party states these results do not show a strongly populated $\pi d_{5/2}$. From where one can conclude that the positioning of the $\pi d_{5/2}$ is well above $\pi g_{7/2}$ in this nucleus, as discussed above. A similar suggestion for ^{136}I can be found in the analysis of [32], coherent with the identification of [6], for the configuration for the 12^- state (about 99% $\pi d_{5/2}$). Therefore, about 2 MeV energy is expected between $\pi d_{5/2}$ and $\pi g_{7/2}$. For the rest of the states with spin/parities of 7^-, 9^- and 11^-, in agreement with our results, their shell-model calculations predicted quite pure $\pi g_{7/2}$ wave functions (70–80%). All states with $I^{\max}$ result from $\nu f_{7/2}$ coupling to $7/2^+$, $11/2^+$, $15/2^+$, and $17/2^+$ of ^{135}I, while due to the extra protons in the isotone ^{138}Cs more fragmented wave functions can be identified. One may note that the missing 10^- experimental state in ^{136}I has been suggested to disappear due to a small $E2$ transition strength with respect to the observed $12^- \rightarrow 11^-$ $M1(+E2)$ [32]. This, as the observation of a similar 6^- isomer in ^{138}Cs with $\pi g^5_{7/2}\nu f_{7/2}$ origin [65], supports the discussed energetically higher positioning of the $\pi d_{5/2}$ orbital also with the increase of Z.

VII. CONCLUSIONS AND SUMMARY

In this work we have measured and extended the excitation level scheme of the ^{136}I nucleus from fission of actinides and from β-decay data. We have identified for the first time several non-yrast states built on the $\nu h_{9/2}\pi f^2_{7/2}h_{11/2}$ and $\nu g^3_{7/2}\pi i_{13/2}$ configurations resulting in most probable spin/parities of (1^+) and (2^+). Large-scale shell-model calculations describe well the experimental data. According to these, the wave functions of the newly observed states are rather pure with small admixtures, indicating the predominantly single-particle excitations in this nucleus. This analysis also suggests little collectivity at the beginning of the $\nu f_{7/2}$ shell for ^{136}I. From our β-decay data from ^{136}Te to ^{136}I we have further enriched the experimental information on the daughter nucleus with observation of several 1^+ states. By a comparison with shell-model predictions, we have identified the GT strength for $A = 136$ and compared it to recent data for $A = 140$ iodine nuclei based on the influence of the $\nu h_{9/2}$ orbital for which we used also β decay data from ^{136}I to ^{136}Xe. We consider that the reproduction of their lowest 1^+ and 2^- populated in GT is successful.

We have confirmed and extended the yrast excitation scheme in ^{136}I in the analysis of fission of actinides. Our data and the observation of the new structures at reasonably high excitation energy suggest a large spacing between the proton orbitals $\pi g_{7/2}$ and $\pi d_{5/2}$, without any particular anomaly suggested earlier, and is consistent with the decrease of this spacing with the increase of N. We have detected new states of spin/parity up to (16^+) and (17^+). These excitations also have rather pure configurations according to our shell-model calculations, which proposes a large energy spacing between the $\nu h_{9/2}$ and $\nu f_{7/2}$ orbitals. In ^{136}I, the high-energy transitions are particularly intense and according to our analysis, possibly represent strong transitions between states with different origins. This means that one has a reasonably large spacing between different configurations, respectively, orbitals involved in these configurations. From the point of view of single-particle excitations, which are possible in ^{136}I between states with different configurations, it is an experimental challenge to identify such transitions in other more exotic nuclei, where currently little or no data is collected.

ACKNOWLEDGMENTS

The authors thank the technical services of the ILL, LPSC, and GANIL for supporting the EXILL campaign and to M. Jentschel for his valuable contribution to the EXILL project.

The EXOGAM collaboration and the INFN Legnaro are acknowledged for the loan of Ge detectors. The authors are indebted for the use of ^{248}Cm to the Office of Basic Energy Sciences, U.S. Dept. of Energy, through the transplutonium element production facilities at the Oak Ridge National Laboratory. R.L. is thankful to Y. Patois for his help in processing grid data analysis. E.S. was partially supported by BNF under Grant No. DFNI-E02/6.

[1] V. Paar, Phys. Lett. B **39**, 466 (1972).
[2] G. Vanden Berghe, Z. Phys. **266**, 139 (1974).
[3] A. Kerek *et al.*, Nucl. Phys. A **195**, 159 (1972).
[4] B. Fogelberg, B. Ekström, L. Sihver, and G. Rudstam, Phys. Rev. C **41**, 1890(R) (1990).
[5] R. A. Meyer *et al.*, Phys. Rev. C **13**, 1617 (1976).
[6] L. Coraggio, A. Covello, A. Gargano, and N. Itaco, Phys. Rev. C **80**, 021305(R) (2009).
[7] K. Li *et al.*, Phys. Rev. C **75**, 044314 (2007).
[8] J. P. Schiffer, S. J. Freeman, J. A. Caggiano, C. Deibel, A. Heinz, C.-L. Jiang, R. Lewis, A. Parikh, P. D. Parker, K. E. Rehm, S. Sinha, and J. S. Thomas, Phys. Rev. Lett. **92**, 162501 (2004).
[9] W. Urban *et al.*, Eur. Phys. J. A **27**, 257 (2006).
[10] R. Lozeva *et al.*, Phys. Rev. C **93**, 014316 (2016).
[11] M.-G. Porquet *et al.*, Eur. Phys. J. A **25**, 319 (2005).
[12] V. Paar *et al.*, Z. Phys. **271**, 11 (1974).
[13] A. Kuriyama *et al.*, Progr. Theor. Phys. **53**, 489 (1975).
[14] T. Rzaca-Urban, M. Czerwinski, W. Urban, A. G. Smith, I. Ahmad, F. Nowacki, and K. Sieja, Phys. Rev. C **88**, 034302 (2013).
[15] W. Urban, W. R. Phillips, I. Ahmad, J. Rekawek, A. Korgul, T. Rzaca-Urban, J. L. Durell, M. J. Leddy, A. G. Smith, B. J. Varley, N. Schulz, and L. R. Morss, Phys. Rev. C **66**, 044302 (2002).
[16] J. Shergur *et al.* (ISOLDE Collaboration), Phys. Rev. C **65**, 034313 (2002).
[17] F. Schussler *et al.*, Z. Phys. A **283**, 43 (1977).
[18] B. Moon *et al.*, Phys. Rev. C **96**, 014325 (2017).
[19] F. F. Hopkins *et al.*, Phys. Rev. C **5**, 1015 (1972).
[20] W. John, F. W. Guy, and J. J. Wesolowski, Phys. Rev. C **2**, 1451 (1970).
[21] L. K. Peker, Nucl. Dat. Sh. **26**, 473 (1979).
[22] http://www.nndc.bnl.gov.
[23] B. Pfeifer, J. Phys. **38**, 9 (1977).
[24] M. Samri *et al.*, Z. Phys. A **321**, 255 (1985).
[25] A. J. Aas, PhD. thesis, University of Oslo, 1999.
[26] P. Bhattacharyya, C. T. Zhang, B. Fornal, P. J. Daly, Z. W. Grabowski, I. Ahmad, T. Lauritsen, L. R. Morss, W. R. Phillips, J. L. Durell, M. J. Leddy, A. G. Smith, W. Urban, B. J. Varley, N. Schulz, E. Lubkiewicz, M. Bentaleb, and J. Blomqvist, Phys. Rev. C **56**, 2363(R) (1997).
[27] A. A. Songozoni, Nucl. Dat. Sh. **95**, 837 (2002).
[28] A. H. Wapstra *et al.*, Nucl. Phys. A **432**, 185 (1985).
[29] G. Audi *et al.*, Nucl. Phys. A **729**, 3 (2003).
[30] U. Keyser *et al.*, in *Proceedings of the 6th International Conference on Atomic Masses and Fundamental Constants* (Plenum Press, New York, 1980), p. 485.
[31] B. Fogelberg, K. A. Mezilev, V. I. Isakov, K. I. Erokhina, H. Mach, E. Ramstrom, and H. Gausemel, Phys. Rev. C **75**, 054308 (2007).
[32] S. H. Liu, J. H. Hamilton, A. V. Ramayya, A. Covello, A. Gargano, N. Itaco, N. J. Stone, A. V. Daniel, J. K. Hwang, Y. X. Luo, J. O. Rasmussen, G. M. Ter-Akopian, S. J. Zhu, and W. C. Ma, Phys. Rev. C **81**, 014316 (2010).
[33] A. Blanc *et al.*, Nucl. Instrum. Methods Phys. Res., Sect. B **317**, 333 (2013).
[34] M. Jentschel *et al.*, J. Instr. **12**, P11003 (2017).
[35] S. Ilieva *et al.*, Phys. Rev. C **94**, 034302 (2016).
[36] R. Lozeva *et al.* (unpublished).
[37] http://www.oecd-nea.org/janis/nea_database.html.
[38] Y. Zheng *et al.*, Phys. Rev. C **87**, 044328 (2013).
[39] P. M. Jones *et al.*, Nucl. Instrum. Methods Phys. Res., Sect. A **362**, 556 (1995).
[40] K. S. Krane, R. M. Steffen, and R. M. Wheeler, Nucl. Data Tables **11**, 351 (1973).
[41] W. D. Hamilton, *The Electromagnetic Interaction in Nuclear Spectroscopy* (North-Holland Publishing Company, Amsterdam, 1975).
[42] W. Urban, K. Sieja, T. Materna, M. Czerwinski, T. Rzaca-Urban, A. Blanc, M. Jentschel, P. Mutti, U. Koster, T. Soldner, G. deFrance, G. S. Simpson, C. A. Ur, C. Bernards, C. Fransen, J. Jolie, J. M. Regis, T. Thomas, and N. Warr, Phys. Rev. C **94**, 044328 (2016).
[43] P. J. Nolan, F. A. Beck, and D. B. Fossan, Ann. Rev. Nucl. Part. Sci. **44**, 561 (1994).
[44] W. Urban *et al.*, Nucl. Phys. A **613**, 107 (1997).
[45] D. Patel *et al.*, J. Phys. G. Nucl. Part. Phys. **28**, 649 (2002).
[46] H. Naïdja, F. Nowacki, and B. Bounthong, Phys. Rev. C **96**, 034312 (2017).
[47] E. Moll *et al.*, Kerntechnik **19**, 374 (1977).
[48] A. Złomaniec, H. Faust, J. Genevey, J. A. Pinston, T. Rzaca-Urban, G. S. Simpson, I. Tsekhanovich, and W. Urban, Phys. Rev. C **72**, 067302 (2005).
[49] T. Kibedi *et al.*, Nucl. Instrum. Methods Phys. Res., Sect. A **589**, 202 (2008).
[50] L. A. Schaller *et al.*, Nucl. Phys. A **165**, 415 (1971).
[51] S. L. Sakharov *et al.*, Nucl. Phys. A **528**, 317 (1991).
[52] I. Ahmad and W. R. Phillips, Rep. Prog. Phys. **58**, 1415 (1995).
[53] P. F. Mantica, B. E. Zimmerman, W. B. Walters, and K. Heyde, Phys. Rev. C **43**, 1696 (1991).
[54] E. Caurier *et al.*, Rev. Mod. Phys. **77**, 427 (2005).
[55] E. Caurier *et al.*, Act. Phys. Pol. B **30**, 705 (1999).
[56] W. Urban *et al.*, Eur. Phys. J. A **5**, 239 (1999).
[57] F. Andreozzi, L. Coraggio, A. Covello, A. Gargano, T. T. S. Kuo, and A. Porrino, Phys. Rev. C **56**, 16(R) (1997).
[58] D. R. Entem and R. Machleidt, Phys. Rev. C **68**, 041001 (2003).
[59] M. Hjorth-Jensen *et al.*, Phys. Rep. **261**, 125 (1995).
[60] H. Naïdja *et al.*, J. Phys.: Conf. Ser. **966**, 012061 (2018).
[61] B. H. Wildental, Phys. Rev. Lett. **22**, 1118 (1969).
[62] T. Rzaca-Urban *et al.*, Phys. Rev. C **75**, 054319 (2007).
[63] R. Lozeva *et al.*, Phys. Rev. C **92**, 024304 (2015).
[64] M. Czerwiński, T. Rzaca-Urban, W. Urban, P. Baczyk, K. Sieja, J. Timar, B. M. Nyakó, I. Kuti, T. G. Tornyi, L. Atanasova, A. Blanc, M. Jentschel, P. Mutti, U. Köster, T. Soldner, G. de France, G. S. Simpson, and C. A. Ur, Phys. Rev. C **93**, 034318 (2016).
[65] L. C. Carras *et al.*, Nucl. Phys. A **171**, 209 (1971).